ORIGINAL ARTICLE

Cellular activation in limbic brain systems during social play behaviour in rats

Linda W. M. van Kerkhof · Viviana Trezza ·
Tessa Mulder · Ping Gao · Pieter Voorn ·
Louk J. M. J. Vanderschuren

Abstract Positive social interactions during the juvenile and adolescent phases of life are essential for proper social and cognitive development in mammals, including humans. During this developmental period, there is a marked increase in peer–peer interactions, signified by the abundance of social play behaviour. Despite its importance for behavioural development, our knowledge of the neural underpinnings of social play behaviour is limited. Therefore, the purpose of this study was to map the neural circuits involved in social play behaviour in rats. This was achieved by examining cellular activity after social play using the immediate early gene c-Fos as a marker. After a session of social play behaviour, pronounced increases in c-Fos expression were observed in the medial prefrontal cortex, medial and ventral orbitofrontal cortex, dorsal striatum, nucleus accumbens core and shell, lateral amygdala, several thalamic nuclei, dorsal raphe and the pedunculopontine tegmental nucleus. Importantly, the cellular activity patterns after social play were topographically organized in this network, as indicated by play-specific correlations in c-Fos activity between regions with known direct connections. These correlations suggest involvement in social play behaviour of the projections from the medial prefrontal cortex to the striatum, and of amygdala and monoaminergic inputs to frontal cortex and striatum. The analyses presented here outline a topographically organized neural network implicated in processes such as reward, motivation and cognitive control over behaviour, which mediates social play behaviour in rats.

L. W. M. van Kerkhof · V. Trezza · T. Mulder ·
L. J. M. J. Vanderschuren
Department of Neuroscience and Pharmacology, Rudolf Magnus
Institute of Neuroscience, University Medical Center Utrecht,
Utrecht, The Netherlands

V. Trezza
Department of Biology, University "Roma Tre", Rome, Italy

P. Gao · P. Voorn
Department of Anatomy and Neurosciences, Neuroscience
Campus Amsterdam, VU University Medical Center,
Amsterdam, The Netherlands

L. J. M. J. Vanderschuren (✉)
Department of Animals in Science and Society, Division of
Behavioural Neuroscience, Faculty of Veterinary Medicine,
Utrecht University, Yalelaan 2, 3584 CM Utrecht, The
Netherlands
e-mail: l.j.m.j.vanderschuren@uu.nl

Abbreviations

AC	Anterior cingulate cortex
AId	Agranular insular cortex dorsal part
AIv	Agranular insular cortex ventral part
BLA	Basolateral amygdala
BNST	Bed nucleus of the stria terminalis
CeA	Central amygdala
CeM	Central medial thalamic nucleus
CL	Central lateral thalamic nucleus
DLO	Dorsolateral orbitofrontal cortex
DRa	Dorsal raphe nucleus anterior level
DRp	Dorsal raphe nucleus posterior level
DS	Dorsal striatum
IL	Infralimbic cortex
IMDl	Intermediodorsal thalamic nucleus lateral part
IMDm	Intermediodorsal thalamic nucleus medial part
LA	Lateral amygdala

lGP	Lateral globus pallidus
LC	Locus coeruleus
lCore	Lateral nucleus accumbens core
LDTg	Laterodorsal tegmental nucleus
LO	Lateral orbitofrontal cortex
lShell	Lateral nucleus accumbens shell
mCore	Medial nucleus accumbens core
MD	Mediodorsal thalamic nucleus
MeA	Medial amygdala
MO	Medial orbitofrontal cortex
mPFC	Medial prefrontal cortex
mShell	Medial nucleus accumbens shell
NaCore	Nucleus accumbens core
NAShell	Nucleus accumbens shell
OFC	Orbitofrontal cortex
OTu	Olfactory tubercle
PC	Paracentral thalamic nucleus
PPTg	Pedunculopontine tegmental nucleus
PrL	Prelimbic cortex
PrLd	Prelimbic cortex dorsal part
PrLv	Prelimbic cortex ventral part
PVl	Paraventricular thalamic nucleus lateral part
PVm	Paraventricular thalamic nucleus medial part
RMTg	Rostromedial tegmental nucleus
SNc	Substantia nigra pars compacta
SNr	Substantia nigra pars reticulata
STR-	Striatal region receiving input from the cortical region mentioned with it
VLO	Ventrolateral orbitofrontal cortex
VO	Ventral orbitofrontal cortex
VP	Ventral pallidum
VS	Ventral striatum
vShell	Ventral nucleus accumbens shell
VTA	Ventral tegmental area

Introduction

The period between weaning and sexual maturity (i.e. childhood and adolescence in humans, roughly equivalent to the juvenile and adolescent stages in rodents) has received widespread attention because of its importance for behavioural development, and conversely, because of the emergence of certain psychiatric disorders during this period (Spear 2000; Paus et al. 2008). During the juvenile and adolescent stages, substantial changes occur in brain and behaviour. In particular, there are profound changes in social behaviour, including increased complexity of the social repertoire and a remarkable increase in peer–peer interactions (Blakemore 2008; Crone and Dahl 2012; Nelson et al. 2005; Spear 2000). For a large part, these peer–peer interactions take the form of social play behaviour. Social play behaviour is one of the earliest forms of non-mother directed social behaviour in mammals (Fagen 1981; Panksepp et al. 1984; Pellis and Pellis 2009; Vanderschuren et al. 1997), although it can also be observed in other species, e.g. reptiles, invertebrates, and avian species (Graham and Burghardt 2010; Pellis and Pellis 2009). Social play behaviour during adolescence is thought to be important for proper social and cognitive development (Baarendse et al. 2013; Panksepp et al. 1984; Pellis and Pellis 2009; Špinka et al. 2001; Van den Berg et al. 1999; Vanderschuren et al. 1997; Von Frijtag et al. 2002). Indeed, abnormalities in play behaviour have been observed in childhood psychiatric disorders such as autism and attention deficit/hyperactivity disorder (Alessandri 1992; Jordan 2003; Manning and Wainwright 2010). In addition, childhood social trauma may have long-lasting repercussions, that last well into adulthood (Braun and Bock 2011). Therefore, in view of its importance for behavioural development, and its relevance for child and adolescent psychiatry, it is essential to identify the neural substrates underlying social play behaviour.

At present, our understanding of the neural substrates of social play behaviour is limited. Clearly, the expression of a complex behaviour such as social play involves a wide array of neural circuits. It has been hypothesized that cortical regions have a role in the facilitation of play behaviour by guiding its expression in the appropriate temporal and contextual settings. In addition, subcortical circuits may mediate the execution of the appropriate locomotor acts and the integration of sensory stimuli, as well as encode the emotional and motivational properties of social play (Pellis and Pellis 2007; Siviy and Panksepp 2011; Vanderschuren et al. 1997).

Neonatal lesion studies have suggested that the cortex is not essential for the execution of social play behaviour itself (Panksepp et al. 1994; Pellis et al. 1992; Schneider and Koch 2005), but that frontal cortical regions are important for the fine-tuning of the expression of social play, such as adapting the play patterns to the partner's behaviour (Bell et al. 2009, 2010; Pellis et al. 2006). Subcortical regions such as the thalamus and striatum have been shown to be important for expression of social play behaviour (Pellis et al. 1993; Siviy and Panksepp 1985, 1987). For example, neonatal depletion of dopamine in the striatum affects the sequential ordering of play patterns (Pellis et al. 1993), while lesions of certain thalamic nuclei, such as the parafascicular nucleus, have been found to reduce social play by disrupting the transmission of somatosensory stimuli related to play (Siviy and Panksepp 1985, 1987). Furthermore, previous immediate early gene expression studies have demonstrated enhanced cellular activity during social play behaviour in brain regions

including the prefrontal cortex, amygdala and striatum (Cheng et al. 2008; Gordon et al. 2002).

Social play behaviour is highly rewarding (Trezza et al. 2011a; Vanderschuren 2010). It is therefore likely that brain regions involved in pleasure and motivation have an important role in this behaviour as well. These regions include the nucleus accumbens and amygdala (Lewis and Barton 2006; Meaney et al. 1981; Trezza et al. 2011b, 2012). Furthermore, several studies have indicated an essential role for monoaminergic neurotransmission in social play behaviour (for review see Trezza et al. 2010). Therefore, it is also likely that activity of monoamine nuclei is altered during social play behaviour.

In the present study, a broad range of the potential neural structures involved in social play behaviour was investigated in male rats. Using expression of the immediate-early-gene c-Fos as a marker, neuronal activity induced by social play behaviour was mapped in the prefrontal cortex, striatum, amygdala, thalamus, pallidum, monoamine nuclei, and tegmental regions providing input into the monoamine nuclei. In addition, it was investigated whether c-Fos activity, induced by social play, correlates between regions known to be connected. This resulted in the identification of a network of brain regions which is activated during social play behaviour in rats.

Materials and methods

Animals

Male Wistar rats (Charles River, Sulzfeld, Germany) arrived in our animal facility at 21 days of age and were housed in groups of four in $40 \times 26 \times 20$ cm Macrolon cages under controlled conditions (i.e. temperature 20–21 °C, 55–65 % relative humidity and 12/12 h light cycle with lights on at 7.00 a.m.). Food and water were available ad libitum. All animals used were experimentally naïve. During the first 6 days, rats were handled at least twice, to familiarize them with the experimenter. All experiments were approved by the Animal Ethics Committee of Utrecht University and were conducted in accordance with Dutch (Wet op de Dierproeven, 1996) and European regulations (Guideline 86/609/EEC).

Behavioural testing

Experiments were performed in a sound-attenuated chamber under dim light conditions, as described previously (Trezza and Vanderschuren 2008; Trezza et al. 2009; Vanderschuren et al. 1995a, b). The test arena was a Plexiglas cage ($40 \times 40 \times 60$ cm) with approximately 2 cm of wood shavings covering the floor. Animals were paired with an unfamiliar test partner. Animals in a test pair did not differ more than 10 g in body weight.

Animals were repeatedly habituated to the test cage (4 consecutive days, 30 min/day) to minimize the influence of novelty of the test environment on the expression of social play behaviour (Trezza and Vanderschuren 2008; Trezza et al. 2009; Vanderschuren et al. 1995a, b) and the induction of c-Fos expression (Badiani et al. 1998; Day et al. 2001; Struthers et al. 2005). The motivation for play was maximally enhanced by isolating the animals 24 h before the test (Niesink and Van Ree 1989; Vanderschuren et al. 1995b, 2008). On the test day, animals were placed in the test cage either in pairs ('play group', 5 pairs, $n = 10$) or alone ('no-play group', $n = 8$) for 15 min, since after social isolation for up to 24 h, rats display most social play behaviour within the first 10–15 min of testing (Trezza and Vanderschuren 2008; Trezza et al. 2009; Vanderschuren et al. 1995a, b). After the test, animals were placed back into their separate cages for 30 min. This survival period was chosen because time course analysis has shown that the expression of stimulus-induced c-Fos mRNA expression peaks in between 30 and 60 min after stimulation (Cullinan et al. 1995; Ostrander et al. 2003). Thus, the animals were killed 45 min after the start of the play session. Subsequently, rats were killed by decapitation, their brains were quickly removed and frozen immediately (−80 °C).

Behaviour of the animals was recorded using a camera with zoom lens, video tape recorder and television monitor. The behaviour of the play group was assessed using the Observer 5.1 software (Noldus Information Technology B.V., The Netherlands). Three behavioural elements were scored (Panksepp et al. 1984; Trezza et al. 2010; Vanderschuren et al. 1997).

- *Frequency of pinning* One animal lying with its dorsal surface on the floor with the other animal is standing over it, which is the most characteristic posture of social play in rats.
- *Frequency of pouncing* One animal attempts to nose or rub the nape of the neck of the partner, which is an index of play solicitation.
- *Time spent in social exploration* One animal sniffing or grooming any part of the partner's body.

c-Fos DIG in situ hybridization

Fresh frozen brains were cryostat sectioned (−20 °C) at 14 μm, mounted on Super-Frost Plus slides (Eric Scientific Co, Portsmouth, NH, USA) and stored at −80 °C. Slides were warmed to room temperature before fixation with 4 % PFA (4 % paraformaldehyde in PBS, 154 mM NaCl, 0.896 mM KH$_2$PO$_4$, 4.58 mM Na$_2$HPO$_4$, pH = 7.5). Acetylation of the slides was performed with acetic

anhydride (0.25 % acetic anhydride in 1.5 % triethanolamine buffer). Subsequently, slides were washed with PBS and 2× saline sodium citrate buffer (SSC buffer) before applying the hybridization mix (50 % formamide, 4× SSC, 0.4 % bakers yeast tRNA, 2 % 50× Denhardt's reagent, 10 % dextran, 0.05 % salmon sperm DNA) containing 5 ng c-Fos probe per section.

The probe was generated using cDNA synthesized from total rat brain RNA and the iScript reverse transcriptase kit with random hexamers, according to manufacturer's protocol (Bio-Rad, Hercules, CA, USA). A PCR was performed with c-Fos-specific primers containing T3/T7 promoters. Primers (Eurogentec, Liège, Belgium) were designed using Primer3 (Rozen and Skaletsky 2000). All primers were checked for gene specificity by BLAST searching. The primer sequences used for c-Fos (Genbank NM_022197.2) were T3 antisense, AATTAACCCTCAC-TAAAGGG-CACAGCCTGGTGAGTTTCAC and T7 sense, GTAATACGACTCACTATAGGG-TCACCCTGC CTCTTCTCAAT. The PCR product size was checked by agarose gel electrophoresis. From these PCR products, labelled probes were generated by linear amplification using the MAXIscript Kit according to manufacturer's protocol (Applied Biosystems, Foster City, CA, USA) and probes were labelled using digoxigenin-UTP (DIG labelling mix, Roche, Penzberg, Germany). The probe size and concentration were checked using agarose gel electrophoreses. The probe was briefly heated at 95 °C before adding it to the hybridization mix and hybridization was performed in a humid chamber at 60 °C overnight.

Post-hybridization washes were carried out with 1× SSC at 60 °C, including a wash with 2× SSC containing RNAse A (0.3 Units/mL, Roche, Penzberg, Germany) at 37 °C. Before antibody incubation, slides were exposed to a blocking solution (1 % blocking powder in TRIS buffer, 100 mM Tris, 150 mM NaCl, pH = 7.5) according to the DIG detection kit manual (Roche, Penzberg, Germany) for 1 h. Slides were incubated with anti-DIG-AP antibody (1:2,500, DIG detection kit, Roche, Penzberg, Germany). This antibody was conjugated to alkaline phosphatase (AP), allowing the use of NBT/BCIP as a substrate to visualize the probe. The antibody incubation was performed overnight at 4 °C.

Following antibody incubation, slides were washed in TBS (100 mM TRIS, 150 mM NaCl, pH = 7.5) and a magnesium buffer (100 mM Tris, 100 mM NaCl, 50 mM MgCl, pH = 9.5). Incubation with the substrate NBT/BCIP (1:50; Roche, Penzberg, Germany) in magnesium buffer was performed in a humid chamber at room temperature for 28 h. The reaction was stopped with TBS containing EDTA (1 mM EDTA, pH = 7.5) and slides were washed twice with water to remove salt precipitate. Slides were left to dry and coverslipped using Merckoglas (Merck, NJ, USA).

Consistency of immunohistochemical staining is of the utmost importance to reliably quantify differences between the play and no-play groups for individual brain regions. Ideally, all tissue sections of the two experimental groups should be hybridized and immunostained within one experiment. Since this is not practically feasible, sections were hybridized and immunostained in separate batches using exactly the same incubation solutions, whereby one labelling batch contained all sections of a given brain region from all animals. For example, all sections containing mPFC and OFC regions were stained simultaneously, to prevent influence of between-batch labelling variation on the data. This approach also allowed for the calculation of correlation coefficients (see below).

Nissl staining

The sections adjacent to those stained for c-Fos were stained with thionin. After fixation with PFA (4 %), slides were placed in thionin solution (0.13 % in aqua bidest). Staining time was optimized for each separate experiment. Subsequently, slides were placed for 1 min in MilliQ water, 70, 80, 96 and 100 % ethanol (3×). Thereafter, slides were placed in xylene 2× for 2 min and coverslipped using Entellan (Merck, NJ, USA).

Tyrosine hydroxylase immunohistochemistry

To determine the borders of the dopaminergic regions, adjacent sections were stained for tyrosine hydroxylase (TH). After fixation with PFA (4 %), slides were washed using TBS and subsequently incubated with a mouse anti-TH antibody (#22941, Incstar, Stillwater, MN, USA) diluted 1:2,000 in TBS-T (TBS with 0.2 % Triton) at 4 °C overnight. The secondary antibody was a biotinylated horse anti-mouse antibody (BA-2000, Vector, Burlingame, CA, USA) and was diluted 1:100 in TBS-T. Slides were incubated with the secondary antibody for 2 h at room temperature. Subsequently, slides were incubated with TBS-T containing the avidin–biotin–peroxidase complex (ABC kit, Thermo Scientific, Waltham, MA, USA) according to the manufactures' protocol and the TH protein was visualized using 3,3′-diaminobenzidine (Sigma, St. Louis, MO, USA) as a substrate (0.005 % in TBS). Afterwards, slides were dehydrated through a series of ascending concentrations of ethanol, transferred to xylene and coverslipped using Entellan (Merck, NJ, USA).

Quantification of c-Fos immunopositive cells

Quantification of c-Fos positive cells was performed as previously described (Nordquist et al. 2008). Images of all regions of interest were digitized using an objective

magnification of 5× on a Leica DM/RBE photomicroscope with a Q-imaging 12 bit camera and MCID software (InterFocus Imaging, Cambridge, UK). Image acquisition was preceded by a flat field correction and a calibration routine to ensure standardized OD values. For each subject 3 (occasionally 2) sections were digitized per region of interest. Sections were made in series of 10; therefore, sections were 140 μM apart.

An overlay was drawn on each image to define the different regions and subregions. Borders of the regions of interest were determined using images of Nissl-stained adjacent sections ("Nissl staining" as described above). Borders were drawn according to the atlas of the rat brain by Paxinos and Watson (1998); these are schematically presented in Fig. 1. An algorithm was used to identify c-Fos positive cells (Nordquist et al. 2008). The
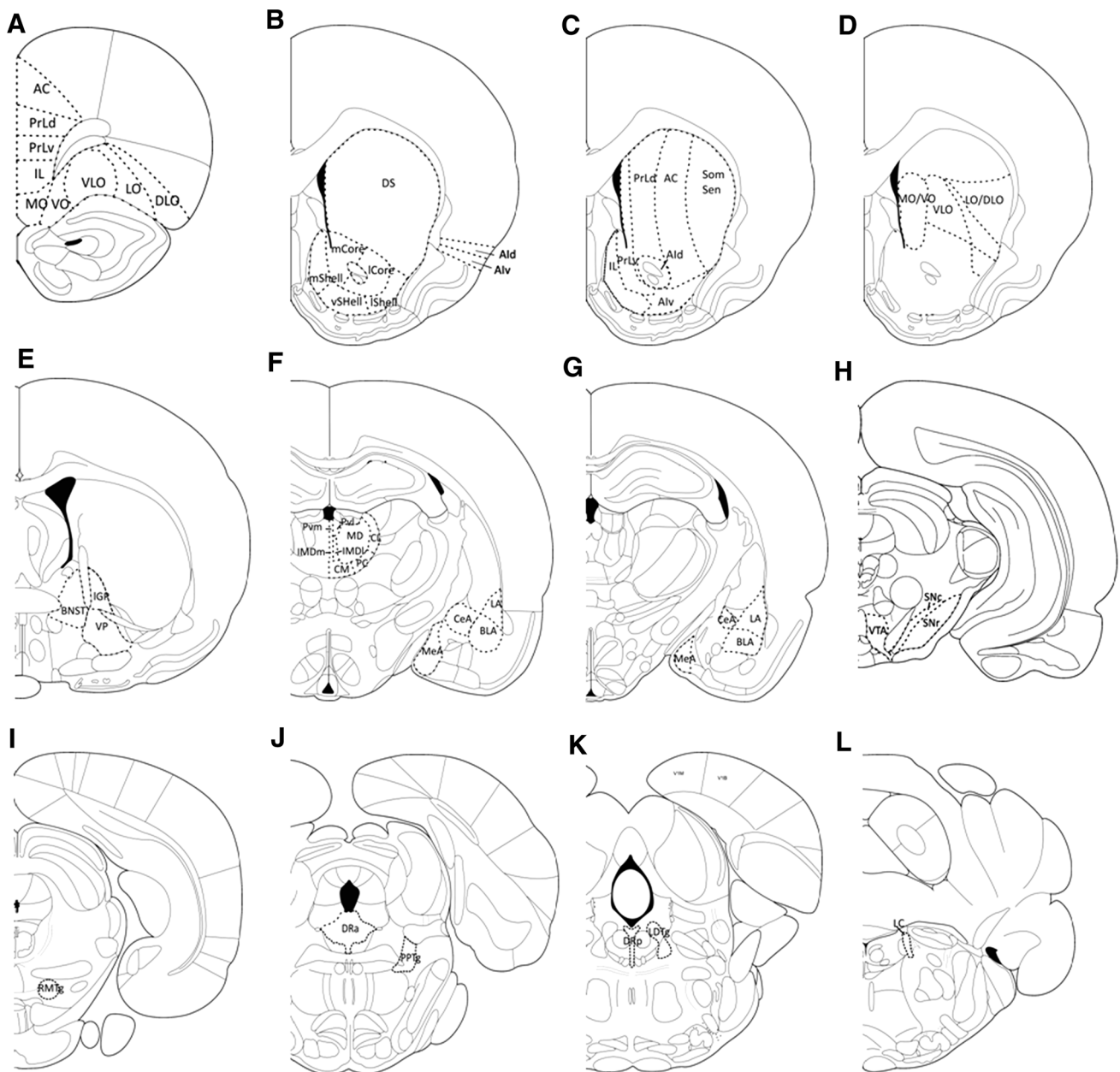
Fig. 1 Schematic representation of the regions in which the c-Fos-positive cells were determined. The regions measured were prefrontal cortex regions at +3.70 mm from Bregma (a), striatal regions at +1.20 mm from Bregma (b–d), lGP and VP at −0.40 mm from Bregma (e), thalamus regions at −2.56 mm from Bregma (f), amygdala regions at −2.56 mm (f) and −3.30 mm (g) from Bregma, VTA and SN at −6.04 mm from Bregma (h), RMTg at −6.72 mm from Bregma (i), PPTg and the anterior part of the DR at −8.00 mm from Bregma (j), the posterior DR and the LDTg at −8.80 mm from Bregma (k), and the LC at −9.68 mm from Bregma (l)

c-Fos-immunopositive cell somata were segregated from background staining using several point operators and spatial filters combined in an algorithm designed to detect local changes in optical density (OD). Images underwent histogram equalization followed by smoothing (low-pass filter, kernel size 7×7). Next, the unfiltered image was subtracted from the smoothed image. Subsequent steps involved optimizing the image for use as a measuring template: the image was binarized and subjected to erosion (kernel size 5×5), smoothing (kernel size 7×7) and dilation (kernel size 3×3). Finally, for detecting objects the size and shape of c-Fos-immunoreactive neurons exclusion criteria were used so that only objects with surface area larger than 8 μm^2, maximum diameter smaller than 8 μm and a form factor smaller than 0.9 were selected. The number of cells counted was corrected with a factor indicating approximate size of a cell, thus preventing two adjacent segmented objects mistakenly counted as one cell. This algorithm allows for an observer-independent measurement. Several parameters were measured: number of c-Fos positive cells, optical density of each cell, total area of each cell, and the total measured surface area of the region. In Figs. 3 and 6 digitized images of sections with c-Fos staining are provided for illustrative purposes. The contrast of these images was enhanced to allow for better visualization (CorelDraw Graphics X5, contrast +60 %, brightness −30 %). The images used in the analysis were not modified.

Data analysis of c-Fos expression levels

The parameters obtained from the MCID software were used to calculate the density of c-Fos positive cells (number of positive cells divided by the total surface area of the region of interest). Changes in (re)activity of a particular brain region upon exposure to a stimulus such as social play not only comprise changes in the number of responsive cells, but also the intensity with which individual cells respond. This intensity can be measured at the cellular level by determining the relative amount of hybridized probe in hybridization histochemistry which represents the amount of mRNA (Higo et al. 1999; Hill et al. 1993; Robbins et al. 1991; Stylianopoulou et al. 2012; Zhao et al. 2008). In the present experiments, we used densitometry to measure the immunocytochemical signal that was used to detect the hybridized c-Fos antisense probe. This signal consists of the purple-brown reaction product generated by alkaline phosphatase in the protocol for detecting digoxigenin-labelled probes as described in the "Materials and methods" section. This method allows for very reliable quantification of hybridization signal, provided that precautions are taken to ensure consistency in the hybridization and immunohistochemical procedures (see "Materials and methods").

To compare the c-Fos-positive cell density in a manner that takes into account cellular response intensity, i.e. the labelling intensity, cells were categorized according to their labelling intensity: light, medium, and dark (see Nordquist et al. 2008). To this end, a frequency histogram of the optical densities of all cells in the no-play group was made for each region of interest. The histograms were used to calculate the 33rd and 67th percentile of the optical density in the no-play group and these optical density values were used to categorize the cells in all animals. The number of cells in each category was divided by the total surface area of the respective region of interest, to determine the cell density per intensity category. The cell densities of the three categories indicate shifts in the frequency histograms of the optical densities (Fig. 2). An upward shift in the histogram would be reflected by an increase in the overall cell density as well as an increase in the medium category and would suggest that social play behaviour recruits a new population of cells. A rightward shift of the curve is expected when the same neurons are active, but express more c-Fos as a result of play behaviour. This would be reflected by an increase in the cell density in the dark category. In a similar fashion, a downward or leftward shift of the histogram would indicate a smaller number of activated cells, or a reduced quantity of c-Fos expression per activated cell.

Statistical analysis

For data analysis, SPSS software 15.0 (IBM software, New York, NY, USA) was used. To determine the effect of a play session on c-Fos-positive cell density, for each animal the mean of three images (taken from three subsequent sections) was calculated for all parameters. Only data from regions for which three intact sections were available were included in the analysis. To assess the effect of a play session on the density of c-Fos-positive cells (FpCD), data were analysed using Student's t test. To determine the effect of play on the FpCD per intensity category a two-way analysis of variance was used, followed by post hoc Student's t test analysis if appropriate.

For the calculation of a correlation coefficient, the average total immunoreactivity for each animal was used, since this parameter takes the number of c-Fos-responsive cells as well as the intensity value of these cells into account. To calculate the total immunoreactivity, the OD value of a detected cell was multiplied with its cell surface, subsequently the sum of these values was calculated per region per section. The mean of three sections was calculated per animal. This average total immunoreactivity per animal was used to calculate the correlation between different regions. For analysis of the correlations a Spearman's correlation test was performed separately per group ('play' and 'no-play').
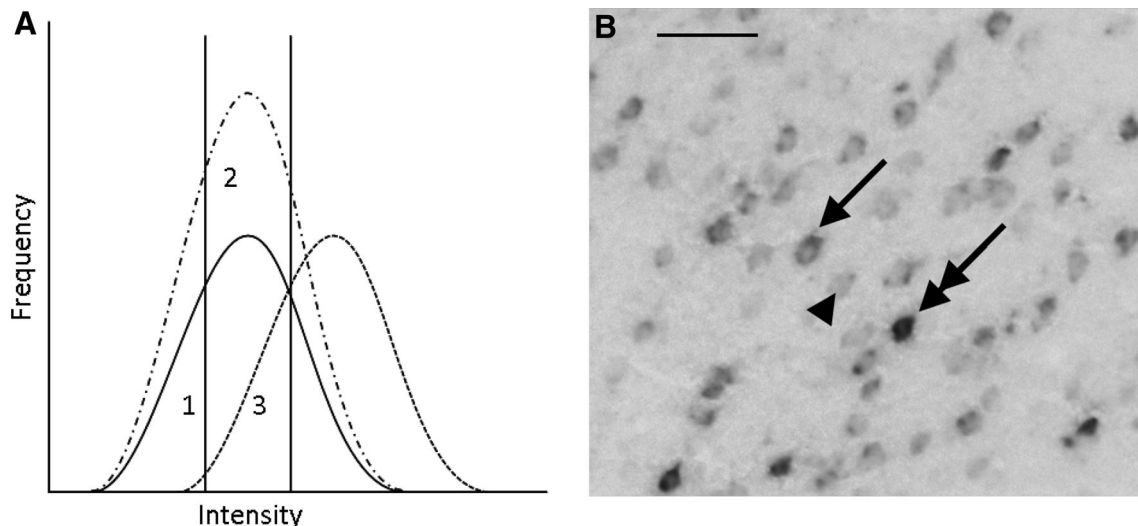
Fig. 2 Theoretical representation of potential shifts in the intensity histogram and an example of differences in optical density of c-Fos positive cells. **a** *Curve 1* indicates the frequency histogram of the control group. The *two vertical lines* indicate the cut-off points used to separate the cells into the light, medium and dark category (33 and 67 %). The area under the curve represents the total number of c-Fos-positive cells per mm^2, i.e. the cell density. If social play behaviour would induce c-Fos activity in a new group of neurons, an increase in the cell density is expected, which would be reflected in an upward shift of the histogram (*curve 2*). This would be reflected in an enhanced cell density primarily in the medium category.

Alternatively, if the same neurons are active, but express more c-Fos as a result of play behaviour, a rightward shift is expected, with an increase in the cell density in the dark category (*curve 3*). In a similar fashion a downward or leftward shift in the histogram could be explained. Adapted from Nordquist et al. (2008). **b** Micrograph depicting c-Fos mRNA probe-immunopositive cells in cortex of a 'play' animal. Cells show different intensities of immunolabelling: dark intensity (*double arrow*), medium intensity (*arrow*) and light intensity (*arrow head*), that fall into the three categories indicated in **a**. *Bar* 100 μm

Results

Expression of social play behaviour

One animal from the 'play' group was excluded from the analysis because of insufficient tissue quality, so that $n = 9$ animals were used in the final analysis. These animals showed on average 33.56 ± 2.32 pins/15 min and the average frequency of pouncing was 52.67 ± 5.21/15 min. The average duration of the time spent on social exploration was 41.29 ± 5.33 s.
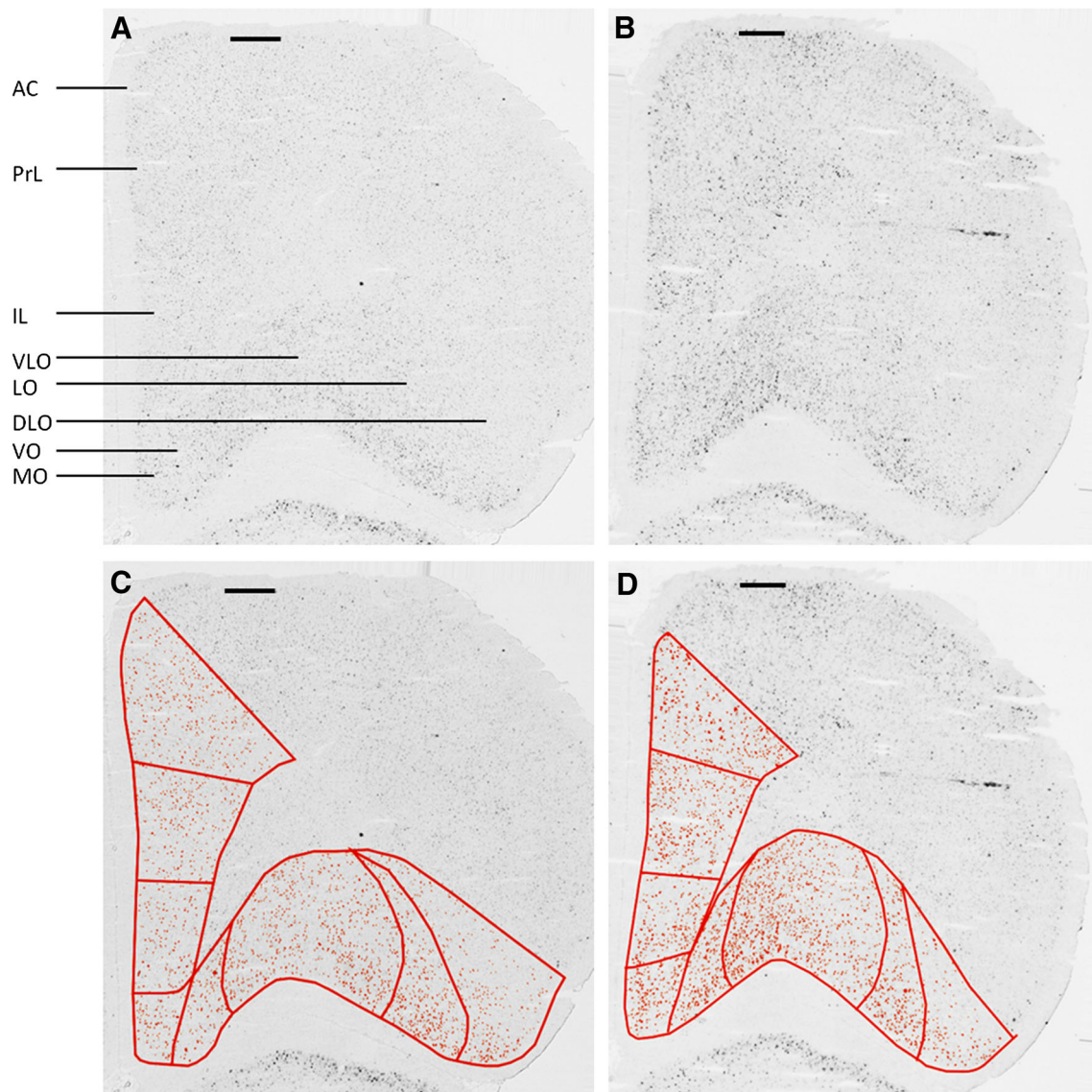
Prefrontal cortex

In prefrontal cortex (Fig. 1a), social play increased the FpCD in the anterior cingulate cortex (AC: $t = 2.639$, $df = 14$, $p = 0.019$), in the dorsal and ventral prelimbic cortex (PrLd: $t = 2.715$, $df = 14$, $p = 0.017$; PrLv: $t = 2.543$, $df = 14$, $p = 0.023$), in the medial orbitofrontal (MO: $t = 2.779$, $df = 12$, $p = 0.017$) and ventrolateral orbitofrontal cortex (VLO: $t = 2.560$, $df = 12$, $p = 0.025$) (Figs. 3, 4). In contrast, social play behaviour decreased the FpCD in the dorsolateral orbitofrontal cortex (DLO: $t = 2.604$, $df = 12$, $p = 0.023$), while no significant effects were observed in the infralimbic cortex (IL: $t = 1.332$, $df = 14$, $p = 0.204$), ventral orbitofrontal cortex (VO: $t = 1.858$, $df = 12$, $p = 0.088$), lateral orbitofrontal cortex (LO: $t = -0.446$, $df = 12$, $p = 0.663$) and in the dorsal and ventral part of the agranular insular cortex (AId: $t = -0.440$, $df = 10.33$, $p = 0.669$; AIv: $t = 1.052$, $df = 8.76$, $p = 0.321$) (Figs. 3, 4).

Analysis of the intensity of immunostaining indicated a difference in the distribution patterns of cellular optical density between the play and no-play groups. We compared the frequencies of optical densities between the two groups by constructing histograms of all c-Fos positive cells per cortical area per group. An example of this approach is shown for anterior cingulate and infralimbic cortex in Fig. 5a–b. Similar histograms were made for the other regions (graphs not shown). All immunostained neurons from the two groups were subsequently divided into three classes on basis of the 33rd and 67th percentile values in the no-play group (Table 1). These classes represent c-Fos-positive cells in the light, medium and dark range of optical density, respectively (see Fig. 2b for examples of these different classes of neurons).

Classifying the c-Fos-immunopositive neurons in the above manner demonstrated that in medial prefrontal cortex the observed increase in the FpCD after play was mainly caused by a rise in the number of reactive cells in the dark intensity category in the AC, PrLd, PrLv and IL (AC: $F_{play \times category}(2,42) = 12.250$, $p < 0.001$;

Fig. 3 Representative pictures of c-Fos mRNA probe-immunostaining in prefrontal cortex of a 'no-play' animal (**a**, **c**) and a 'play' animal (**b**, **d**). The micrographs in **a** and **b** are modified versions of the original, digitized images used for quantification. The contrast of these images was enhanced to allow for better visualization (Corel-Draw Graphics X5, contrast +60 %, brightness −30 %). The images used in the analysis were not modified. **c** and **d** show the same images as **a** and **b** including an overlay of segmented, counted and measured c-Fos positive cell bodies. **c** and **d** also show the boundaries of the individual cortical regions (as described in the text and in Fig. 1). *AC* anterior cingulate cortex, *PrL* prelimbic cortex, *IL* infralimbic cortex, *VLO* ventrolateral orbitofrontal cortex, *LO* lateral orbitofrontal cortex, *DLO* dorsolateral orbitofrontal cortex, *VO* ventral orbitofrontal cortex, *MO* medial orbitofrontal cortex. *Bar* 500 μm

$t_{light} = -1.702$, $df = 14$, $p = 0.111$; $t_{medium} = 1.232$, $df = 14$, $p = 0.238$; $t_{dark} = 4.109$, $df = 14$, $p = 0.001$; PrLd: $F_{play \times category}$ (2,42) = 12.670, $p < 0.001$; $t_{light} = -1.630$, $df = 14$, $p = 0.125$; $t_{medium} = -0.499$, $df = 14$, $p = 0.625$; $t_{dark} = 3.646$, $df = 14$, $p = 0.003$; PrLv: $F_{play \times category}$ (2,42) = 7.609, $p = 0.002$; $t_{light} = -1.183$, $df = 14$, $p = 0.256$; $t_{medium} = 0.314$, $df = 14$, $p = 0.758$; $t_{dark} = 2.876$, $df = 14$, $p = 0.012$; IL: $F_{play \times category}$(2,42) = 4.379, $p = 0.019$; $t_{light} = -0.863$, $df = 14$, $p = 0.402$; $t_{medium} = -0.373$, $df = 14$, $p = 0.715$; $t_{dark} = 2.331$, $df = 14$, $p = 0.035$). The observed increase in overall FpCD (except for the IL) together with a specific increase in the dark category and no significant changes in the light and medium categories reflects a rightward shift of the OD value distribution. This suggests that the same population of neurons that is active in the no-play group is expressing more c-Fos after play (Table 1; see Fig. 5a, b for frequency histograms of the AC and IL, respectively). In addition, more cells may now have reached the detection threshold since minor, non-significant changes were present in the light-intensity range and virtually no changes in the medium range.
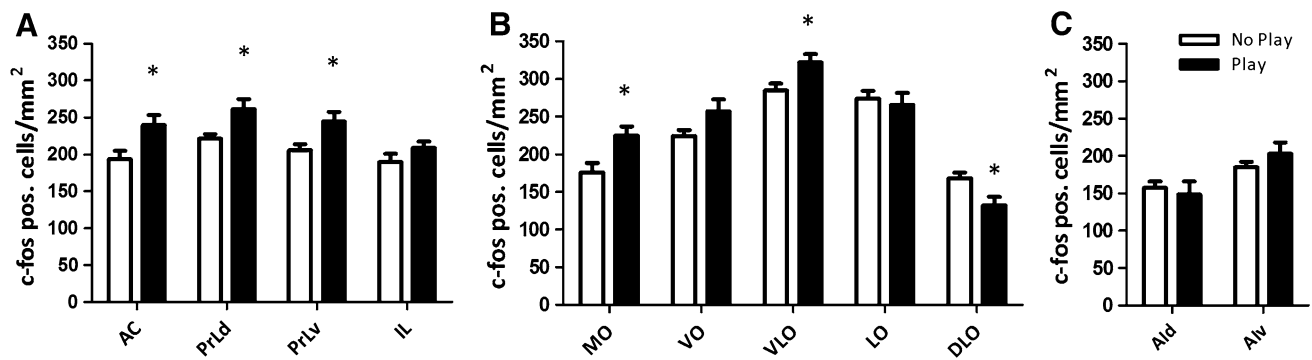
Fig. 4 Social play behaviour affected the c-Fos positive cell density in prefrontal regions. The c-Fos-positive cell density was determined in rats after receiving a play session ('play' group) and in rats that were placed in the test cage without a partner present ('no-play' group). Regions measured include medial prefrontal regions (**a**), orbitofrontal regions (**b**) and agranular insular cortical regions (**c**). Data are presented as mean ± SEM. *$p < 0.05$, different from the no-play group. *AC* anterior cingulate cortex, *PrLd* prelimbic cortex dorsal part, *PrLv* prelimbic cortex ventral part, *IL* infralimbic cortex, *MO* medial orbitofrontal cortex, *VO* ventral orbitofrontal cortex, *VLO* ventrolateral orbitofrontal cortex, *LO* lateral orbitofrontal cortex, *DLO* dorsolateral orbitofrontal cortex, *AId* agranular insular cortex dorsal part, *AIv* agranular insular cortex ventral part
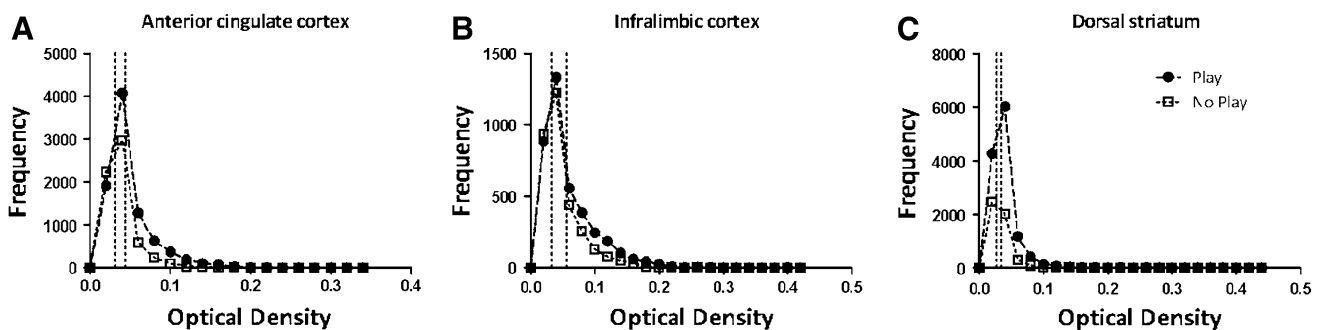
Fig. 5 Frequency histograms of the optical density of measured c-Fos positive cells used to categorize cells into light, medium, or dark categories. The *dotted lines* indicate the 33rd and 67th percentiles, i.e. the border between light and medium and between medium and dark cells. In the anterior cingulate cortex (**a**) and infralimbic cortex (**b**), significantly more dark cells are present after a play session (see also Table 1). In contrast, in the dorsal striatum (**c**) in all three optical density categories more cells are detected after a play session (see also Table 1)

In the orbitofrontal cortex, a response similar to that in medial prefrontal cortex was seen in VLO, VO and MO (Table 1), pointing to a rightward shift in the OD distribution (MO: $F_{\text{play}\times\text{category}}(2,36) = 5.939$, $p < 0.001$; $t_{\text{light}} = -0.278$, $df = 12$, $p = 0.786$; $t_{\text{medium}} = 0.416$, $df = 12$, $p = 0.686$; $t_{\text{dark}} = 6.521$, $df = 12$, $p = 0.013$; VLO: $F_{\text{play}\times\text{category}}(2,36) = 13.366$, $p < 0.001$; $t_{\text{light}} = -2.121$, $df = 12$, $p = 0.055$; $t_{\text{medium}} = -0.667$, $df = 12$, $p = 0.517$; $t_{\text{dark}} = 3.571$, $df = 12$, $p = 0.004$; VO: $F_{\text{play}\times\text{category}}(2,36) = 5.939$, $p = 0.006$; $t_{\text{light}} = -0.912$, $df = 12$, $p = 0.380$; $t_{\text{medium}} = 0.751$, $df = 12$, $p = 0.467$; $t_{\text{dark}} = 2.924$, $df = 12$, $p = 0.013$). However, DLO and LO reacted differently to play, because a significant decrease was observed in both regions in the light (DLO and LO) and medium (LO) classes of c-Fos-positive neurons which was accompanied by non-significant increases in the dark cell category (DLO: $F_{\text{play}\times\text{category}}(2,39) = 3.561$, $p = 0.038$; $t_{\text{light}} = -2.410$, $df = 13$, $p = 0.031$;

$t_{\text{medium}} = -1.434$, $df = 13$, $p = 0.175$; $t_{\text{dark}} = 1.213$, $df = 13$, $p = 0.247$; LO: $F_{\text{play}\times\text{category}}(2,36) = 6.896$, $p = 0.003$; $t_{\text{light}} = -3.076$, $df = 12$, $p = 0.010$; $t_{\text{medium}} = -2.327$, $df = 12$, $p = 0.038$; $t_{\text{dark}} = 1.839$, $df = 12$, $p = 0.091$) (Table 1). Clearly, in DLO and LO, the histogram of OD values in the play group was skewed to the right side, with a loss of cells in the light and medium staining intensity ranges. These cells apparently did no longer reach the detection limit, whereas the population expressing large amounts of c-Fos—the darkly labelled cells—remained intact.

In the agranular insular cortex, changes in FpCD followed the same pattern as in the DLO and LO. In both AIv and AId, the number of lightly immunostained cells was decreased after a play session (AId: $F_{\text{play}\times\text{category}}(2,42) = 4.145$, $p = 0.023$; $t_{\text{light}} = -3.048$, $df = 13$, $p = 0.009$; $t_{\text{medium}} = -0.920$, $df = 13$, $p = 0.375$; $t_{\text{dark}} = 1.312$, $df = 13$, $p = 0.212$; AIv: $F_{\text{play}\times\text{category}}(2,42) = 3.995$, $p = 0.026$;

Table 1 The c-Fos-positive cell density induced by social play behaviour divided into three categories of intensity levels (light, medium, dark)

Region	Subregion	Group	Light	Medium	Dark
Medial prefrontal cortex	AC	No play	64.38 (±7.99)	64.26 (±3.11)	64.84 (±8.05)
		Play	49.63 (±3.37)	72.75 (±6.14)	117.35 (±9.92)**
	PrLd	No play	71.39 (±6.40)	74.28 (±2.84)	75.43 (±8.88)
		Play	54.71 (±7.98)	72.44 (±2.36)	134.13 (±13.43)**
	PrLv	No play	66.05 (±6.32)	69.35 (±2.81)	69.12 (±7.74)
		Play	56.72 (±4.72)	70.86 (±3.89)	116.97 (±12.69)*
	IL	No play	62.12 (±7.74)	63.83 (±2.47)	63.60 (±9.15)
		Play	53.33 (±6.61)	62.23 (±3.51)	92.80 (±8.56)*
Orbitofrontal cortex	MO	No play	58.33 (±6.84)	60.46 (±5.25)	57.09 (±5.03)
		Play	55.57 (±7.18)	63.04 (±3.28)	106.06 (±5.57)***
	VO	No play	73.80 (±6.88)	73.83 (±3.79)	76.76 (±7.87)
		Play	63.91 (±8.38)	77.60 (±3.29)	115.61 (±10.70)*
	VLO	No play	94.90 (±5.31)	94.78 (±4.36)	95.63 (±10.59)
		Play	68.39 (±5.31)	91.39 (±2.65)	162.23 (±15.35)**
	LO	No play	93.15 (±5.60)	92.06 (±3.58)	88.88 (±9.99)
		Play	65.65 (±6.97)*	78.11 (±4.81)*	122.05 (±15.02)
	DLO	No play	56.47 (±7.01)	56.47 (±4.06)	55.06 (±8.10)
		Play	35.20 (±4.95)*	44.59 (±7.57)	69.75 (±9.05)
Agranular insular cortex	AIv	No play	61.55 (±6.78)	62.51 (±3.63)	60.81 (±7.41)
		Play	44.12 (±4.39)*	64.17 (±5.26)	82.87 (±11.02)
	AId	No play	51.87 (±5.88)	52.77 (±3.63)	52.49 (±6.08)
		Play	31.31 (±3.68)*	46.93 (±4.98)	70.46 (±11.62)
Striatum	Core	No play	13.00 (±1.36)	13.48 (±1.36)	13.23 (±1.60)
		Play	11.98 (±1.10)	18.88 (±1.17)*	23.65 (±3.28)*
	mCore	No play	13.70 (±1.05)	15.18 (±1.51)	15.90 (±2.43)
		Play	11.98 (±0.62)	19.32 (±1.87)	26.90 (±5.89)
	lCore	No play	12.74 (±1.89)	13.13 (±0.73)	14.15 (±1.17)
		Play	12.02 (±2.12)	17.45 (±0.70)**	20.50 (±3.21)**
	Shell	No play	18.31 (±1.12)	18.93 (±1.58)	18.27 (±1.39)
		Play	14.42 (±1.38)	22.90 (±1.39)	29.46 (±3.71)*
	mShell	No play	17.73 (±1.58)	18.94 (±2.00)	21.33 (±5.68)
		Play	14.24 (±1.47)	22.01 (±1.80)*	26.48 (±4.12)*
	vShell	No play	18.27 (±1.27)	19.29 (±1.75)	19.39 (±2.78)
		Play	16.36 (±1.98)	23.16 (±2.45)	26.31 (±4.61)
	lShell	No play	21.01 (±2.29)	20.89 (±1.55)	22.30 (±3.07)
		Play	19.59 (±2.76)	25.09 (±1.67)	30.26 (±3.65)
	DS	No play	10.02 (±0.85)	10.39 (±1.09)	10.29 (±1.09)
		Play	12.58 (±0.75)*	21.67 (±1.01)**	31.86 (±3.79)***
	Otub	No play	33.67 (±2.61)	34.28 (±3.46)	34.34 (±4.01)
		Play	22.12 (±2.33)**	33.21 (±2.60)	45.74 (±6.92)
Cortical inputs to the striatum	STR-SomSen	No play	7.46 (±0.071)	7.41 (±0.84)	7.46 (±0.059)
		Play	11.70 (±0.69)***	21.97 (±1.38)***	37.95 (±3.46)***
	STR-AC	No play	10.79 (±1.13)	11.27 (±1.08)	10.98 (±1.13)
		Play	12.30 (±1.35)	22.73 (±1.43)*	29.02 (±3.23)*
	STR-PrLd	No play	13.73 (±1.07)	14.15 (±1.96)	13.92 (±1.90)
		Play	12.15 (±0.70)	18.64 (±1.94)	27.32 (±3.25)*

Table 1 continued

Region	Subregion	Group	Light	Medium	Dark
	STR-PrLv	No play	13.21 (±1.15)	13.50 (±1.55)	13.32 (±1.99)
		Play	11.02 (±0.86)	19.52 (±1.70)	26.70 (±4.38)*
	STR-IL	No play	22.02 (±2.22)	21.91 (±2.68)	21.79 (±2.18)
		Play	14.96 (±1.63)*	21.09 (±2.23)	32.70 (±4.81)
	STR-AIv	No play	33.09 (±2.08)	32.93 (±3.45)	33.65 (±3.97)
		Play	22.96 (±2.46)*	34.15 (±2.33)	44.67 (±6.39)
	STR-AId	No play	12.22 (±1.87)	11.95 (±1.09)	11.61 (±1.16)
		Play	7.83 (±0.59)	13.95 (±1.34)	18.38 (±2.74)
	STR-MO/VO	No play	11.15 (±0.73)	11.57 (±1.60)	10.96 (±1.73)
		Play	11.07 (±0.78)	14.19 (±1.84)	25.42 (±6.61)
	STR-VLO	No play	10.12 (±1.34)	10.46 (±1.25)	10.16 (±1.20)
		Play	12.98 (±1.17)	20.28 (±1.11)***	25.91 (±2.79)***
	STR-LO/DLO	No play	7.22 (±0.59)	7.10 (±0.91)	7.11 (±0.63)
		Play	10.23 (±1.05)*	20.45 (±1.56)***	34.17 (±3.05)***
Amygdala −2.56 mm from Bregma	LA	No play	30.35 (±2.87)	30.51 (±2.72)	27.37 (±3.80)
		Play	22.77 (±3.31)	40.47 (±2.73)*	45.20 (±6.27)*
	BLA	No play	37.34 (±4.31)	35.77 (±3.03)	29.39 (±5.12)
		Play	28.31 (±3.91)	40.70 (±4.52)	49.68 (±6.78)*
	CeA	No play	11.29 (±1.31)	11.63 (±1.09)	10.31 (±3.29)
		Play	11.94 (±2.59)	17.76 (±4.00)	30.52 (±12.82)
	MeA	No play	24.46 (±2.51)	27.89 (±2.23)	24.43 (±4.46)
		Play	23.67 (±1.47)	30.74 (±2.46)	39.41 (±6.02)
Amygdala −3.30 mm from Bregma	LA	No play	48.95 (±3.04)	47.74 (±3.85)	41.25 (±6.49
		Play	47.65 (±7.81)	53.67 (±4.93)	57.58 (±5.40)
	BLA	No play	26.32 (±3.05)	27.89 (±1.60)	26.72 (±2.40)
		Play	26.74 (±4.08)	31.23 (±3.42)	34.01 (±3.26)
	CeA	No play	25.36 (±3.77)	28.13 (±4.55)	30.50 (±8.10)
		Play	31.92 (±5.21)	30.42 (±5.49)	33.99 (±9.12)
	MeA	No play	34.10 (±5.08)	33.43 (±3.47)	32.48 (±4.38)
		Play	26.89 (±5.75)	33.72 (±8.41)	44.92 (±7.28)
BNST	BNST	No play	7.44 (±1.54)	8.19 (±0.90)	7.70 (±1.02)
		Play	8.38 (±2.22)	11.42 (±1.42)	16.05 (±1.57)
Thalamus	MD	No play	57.89 (±7.67)	57.74 (±2.03)	54.84 (±9.31)
		Play	66.25 (±7.37)	60.57 (±7.80)	55.21 (±11.57)
	CL	No play	66.84 (±7.18)	68.32 (±7.05)	64. 83 (±10.62)
		Play	82.98 (±9.68)	68.63 (±7.56)	64.16 (±9.74)
	PC	No play	62.75 (±6.36)	67.10 (±4.10)	64.91 (±11.28)
		Play	75.11 (±11.20)	81.71 (±9.01)	78.39 (±11.92)
	CeM	No play	83.49 (±7.45)	86.72 (±6.97)	87.95 (±13.66)
		Play	94.07 (±11.51)	104.79 (±8.92)	104.51 (±17.65)
	IMDl	No play	37.12 (±7.14)	36.55 (±5.30)	41.21 (±9.53)
		Play	40.01 (±7.16)	51.02 (±5.95)	91.37 (±18.58)
	IMDm	No play	67.69 (±8.28)	66.29 (±6.25)	67.74 (±7.53)
		Play	60.60 (±8.97)	70.37 (±9.62)	89.54 (16.66)
	PVl	No play	53.11 (±8.45)	53.19 (±4.56)	56.17 (±10.25)
		Play	51.64 (±8.56)	81.53 (±9.43)	56.15 (±10.51)
	PVm	No play	82.93 (±10.66)	84.15 (±6.54)	80.69 (±10.19)
		Play	86.77 (±7.85)	86.64 (±11.71)	83.36 (±9.89)

Table 1 continued

Region	Subregion	Group	Light	Medium	Dark
Pallidum	lGP	No play	5.97 (±1.47)	5.59 (±1.45)	6.34 (±1.54)
		Play	1.51 (±0.48)	3.91 (±0.99)	5.13 (±0.63)
	VP	No play	8.59 (±2.18)	9.20 (±1.35)	9.20 (±1.54)
		Play	6.17 (±1.01)	8.10 (±0.99)	7.24 (±1.20)
VTA/SN	VTA	No play	11.38 (±1.08)	11.70 (±1.22)	11.57 (±1.23)
		Play	9.17 (±1.17)	11.62 (±1.62)	12.64 (±2.50)
	SNc	No play	11.76 (±2.06)	11.92 (±2.04)	12.31 (±1.83)
		Play	8.96 (±1.54)	9.54 (±0.86(	16.64 (±1.61)
	SNr	No play	9.74 (±0.97)	9.95 (±1.50)	9.93 (±1.39)
		Play	8.77 (±0.80)	9.76 (±1.24)	10.74 (±1.50)
DR	DRa	No play	19.59 (±5.96)	22.15 (±3.93)	21.52 (±5.05)
		Play	20.39 (±6.75)	26.31 (±2.43)	52.10 (±11.79)
	DRp	No play	15.37 (±2.75)	15.85 (±1.94)	15.76 (±2.83)
		Play	20.95 (±6.75)	19.91 (±2.79)	21.58 (±3.65)
LC	LC	No play	21.33 (±4.81)	18.58 (±2.77)	20.77 (±5.82)
		Play	28.87 (±8.34)	19.91 (±2.79)	19.88 (±6.88)
Tegmentum regions	RMTg	No play	10.31 (±3.72)	9.27 (±1.43)	8.94 (±1.80)
		Play	2.80 (±0.71)	9.06 (±1.18)	15.07 (±1.43)*
	LDTg	No play	16.66 (±3.50)	15.62 (±2.39)	14.90 (±3.36)
		Play	27.25 (±6.44)	25.92 (±4.26)	26.52 (±6.65)
	PPTg	No play	15.48 (±4.18)	13.55 (±2.43)	12.43 (±1.94)
		Play	28.19 (±6.74)	22.19 (±2.94)	16.73 (±13.25)

The c-Fos positive cell density was determined in rats after receiving a play session ('play' group) and in rats that were placed in the test cage without a partner present ('no-play' group). All regions measured are included and data are presented as the mean ± SEM

* $p < 0.05$, ** $p < 0.01$, *** $p < 0.001$, different from the no-play group

$t_{light} = -2.214$, $df = 13$, $p = 0.045$; $t_{medium} = 0.252$, $df = 13$, p = 0.805; $t_{dark} = 1.611$, $df = 13$, $pp = 0.131$) (Table 1). The number of cells in the medium-intensity category was not affected and the darkly stained class of cells showed no significant changes with a tendency for increase. The play session had apparently resulted in a loss of light to medium-intensity cells, similar to the response in DLO and LO.

In summary, social play induced c-Fos expression in several prefrontal regions. The most pronounced effects were observed in the dorsal region of the mPFC (AC and PrL), and medial/ventral part of the OFC (including the MO and VLO). Taking the cellular response intensities into account, a distinction can be made between AC, PrL, MO, VO and VLO on the one hand, and LO, DLO, AIv and AId on the other.
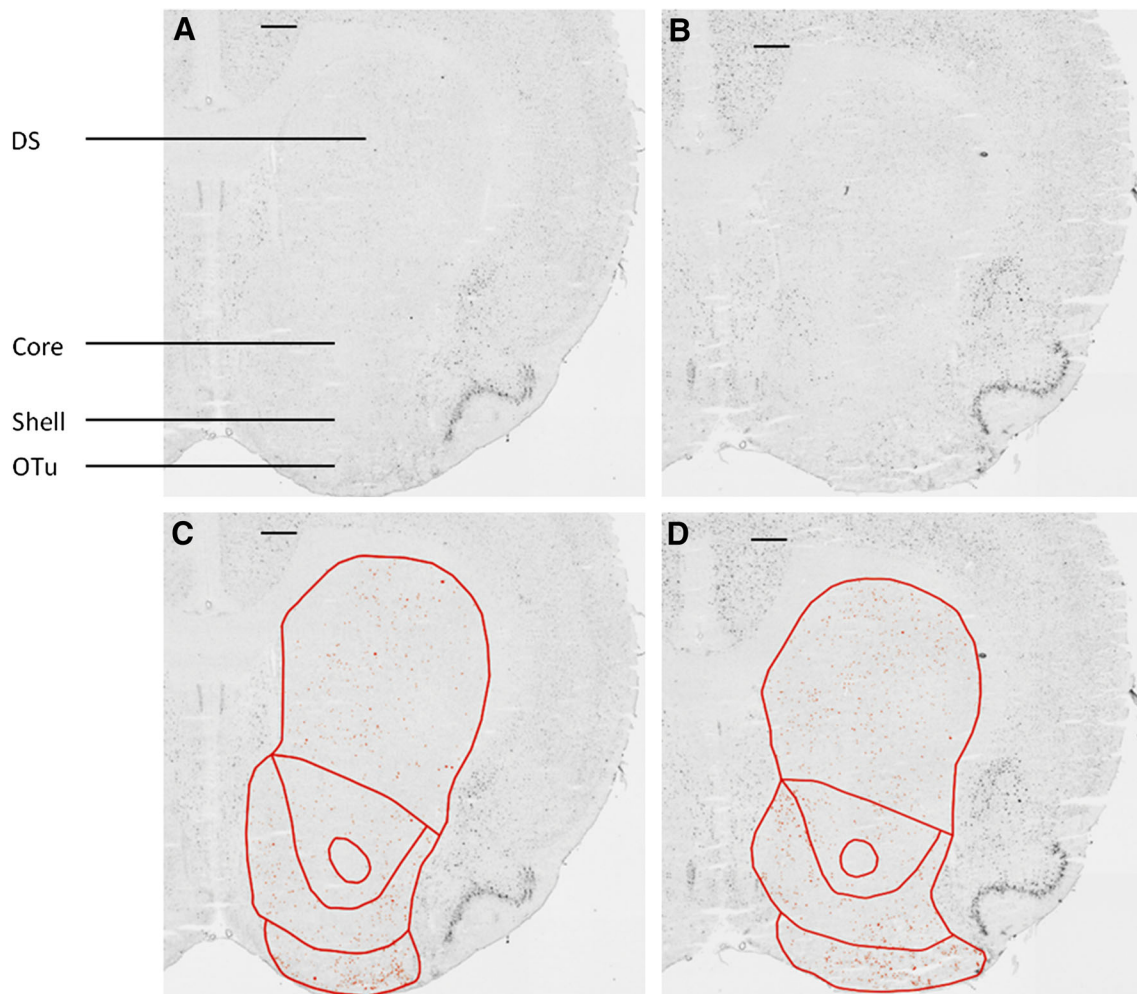
Striatum

To determine involvement of the striatum in social play behaviour, the FpCD was analysed in several striatal sub-regions (Figs. 1b, 6, 7). The nucleus accumbens core and shell were measured as a whole and divided into different

subregions [NaCore: medial (mCore) and lateral part (lCore); NaShell: medial (mShell), ventral (vShell), and lateral part (lShell)], because anatomical and functional differences have been reported in subdivisions of the Na-Core and NaShell (van der Plasse et al. 2012; Voorn et al. 2004; Willuhn et al. 2003). In the NaCore, an increase in the FpCD was observed (NaCore: $t = 2.707$, $df = 13$, $p = 0.018$; Fig. 7a). This increase was clearly present in the lCore ($t = 2.831$, $df = 13$, $p = 0.014$), while in the mCore a trend towards an increase was observed ($t = 2.109$, $df = 13$, $p = 0.055$) (Fig. 7a). Social play behaviour also enhanced the FpCD in the NaShell ($t = 2.194$, $df = 13$, $p = 0.047$; Fig. 7b). This increase was found in the mShell ($t = 2.271$, $df = 13$, $p = 0.041$) and a trend towards an increase was observed in the lShell ($t = 2.107$, $df = 9.19$, $p = 0.064$) (Fig. 7b). In the vShell, no effects of social play were observed ($tt = 1.287$, $df = 13$, $p = 0.220$). A large increase in FpCD after social play was observed in the dorsal striatum (DS; $t = 6.997$, $df = 10.8$, $p < 0.001$), but not in the olfactory tubercle (OTu; $t = 0.110$, $df = 13$, $p = 0.914$; Fig. 7c).

Dividing the c-Fos positive cells into three different categories based on intensity levels (Table 1), showed that

Fig. 6 Representative digitized images of c-Fos mRNA probe-immunostaining in the striatum of a 'no-play' animal (**a**, **c**) and a 'play' animal (**b**, **d**). The micrographs in **a** and **b** are modified versions of the original, digitized images used for quantification. The contrast of these images was enhanced to allow for better visualization (CorelDraw Graphics X5, contrast +60 %, brightness −30 %). The images used in the analysis were not modified. **c** and **d** show the same images including overlays outlining the individual striatal regions and the segmented c-Fos-positive cells. *DS* dorsal striatum, *Core* nucleus accumbens core, *Shell* nucleus accumbens shell, *OTu* olfactory tubercle. *Bar* 500 μm

in the NaCore, the lCore, the Shell and the mShell enhancement of the FpCD was present mainly in the medium and dark categories (NaCore, $F_{\text{play}\times\text{category}}(2,39) = 3.914, p = 0.028$; $t_{\text{light}} = -0.588$, $df = 13$, $p = 0.567$; $t_{\text{medium}} = 3.027$, $df = 13, p = 0.010$; $t_{\text{dark}} = 2.581$, $df = 9.341$, $p = 0.032$; lCore $F_{\text{play}\times\text{category}}(2,39) = 2.991$, $p = 0.042$; $t_{\text{light}} = -0.353$, $df = 13$, $p = 0.730$; $t_{\text{medium}} = 4.240$, $df = 13$, $p = 0.001$; $t_{\text{dark}} = 3.099$, $df = 13$, $p = 0.008$; NaShell, $F_{\text{play}\times\text{category}}(2,39) = 6.767$, $p = 0.003$; $t_{\text{light}} = -2.143, df = 13, p = 0.052; t_{\text{medium}} = 1.896, df = 13, p = 0.080$; $t_{\text{dark}} = 2.826$, $df = 8.909$, $p = 0.020$; mShell, $F_{\text{play}\times\text{category}}(2,39) = 6.408$, $p = 0.004$; $t_{\text{light}} = -1.457$, $df = 13$, $t_{\text{medium}} = 2.174$, $df = 13$, $p = 0.049$; $t_{\text{dark}} = 2.914$, $df = 13$, $p = 0.012$). Although no significant changes were observed in mCore, vShell and lShell

(mCore: $F_{\text{play}\times\text{category}}(2,39) = 2.991$, $p = 0.062$; vShell: $F_{\text{play}\times\text{category}}(2,39) = 2.415, p = 0.103$; lShell: $F_{\text{play}\times\text{category}}(2,39) = 3.029$, $p = 0.061$), the cell density values in the medium and dark classes show a similar trend toward an increase. Comparable to the medial prefrontal cortex and the MO, VO and VLO subregions of the orbitofrontal cortex, the number of cells in the light-intensity category in the various subregions of nucleus accumbens was lower after social play. However, this decrease in lightly immunostained cell density did not reach significance, neither in nucleus accumbens nor, as described above, in frontal cortex. These changes in nucleus accumbens point to a cellular response that resembles the response to social play in medial prefrontal cortex and the aforementioned subregions of orbitofrontal cortex: a rightward shift of the OD value distribution with increases in total
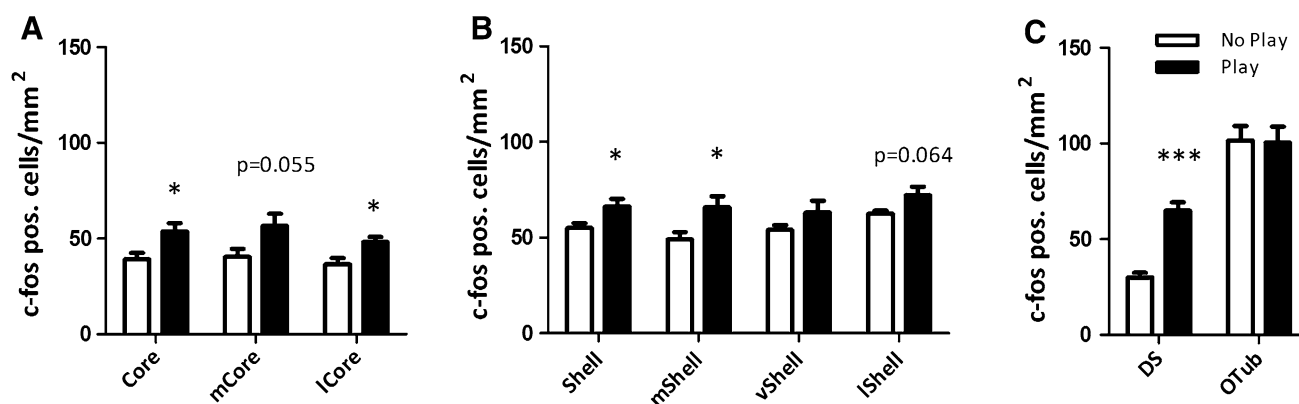
Fig. 7 Social play-induced c-Fos activity in dorsal and ventral striatum. The c-Fos-positive cell density was determined in rats after receiving a play session ('play' group) and in rats that were placed in the test cage without a partner present ('no-play' group). Regions measured include the nucleus accumbens core subregions (a), nucleus accumbens shell regions (b), and the dorsal striatum and olfactory tubercle (c). Data are presented as mean ± SEM. *$p < 0.05$,

***$p < 0.001$, different from the no-play group. Core nucleus accumbens core, mCore medial nucleus accumbens core, lCore lateral nucleus accumbens core, Shell nucleus accumbens shell, mShell medial nucleus accumbens shell, vShell ventral nucleus accumbens shell, lShell lateral nucleus accumbens shell, DS dorsal striatum, OTub olfactory tubercle

number of c-Fos immunopositive cells that reach significance in both Core and Shell, particularly in lCore and mShell.

After classifying the c-Fos-positive neurons in three classes of staining intensity, DS shows responses after social play that are different from the patterns seen in nucleus accumbens. In DS, a significant increase was found in density of c-Fos-positive cells in all three categories ($F_{play \times category}(2,39) = 12.900$, $p < 0.001$; $t_{light} = 2.265$, $df = 13$, $p = 0.041$; $t_{medium} = 7.573$, $df = 13$, $p < 0.001$; $t_{dark} = 5.475$, $df = 8.139$, $p = 0.001$) (Table 1). The frequency histogram of the DS is shown in Fig. 5c. These results indicate that the population distribution of c-Fos cells in DS shows an upward shift after social play, suggesting that a new population of reactive neurons is recruited.

In contrast to the other striatal subregions, the OTu displays a significant reduction of the FpCD in the light cell category, with no changes in the medium category and a non-significant increase in the dark cell category ($F_{play \times category}(2,39) = 3.977$, $p = 0.027$; $t_{light} = -3.306$, $df = 13$, $p = 0.006$; $t_{medium} = -0.252$, $df = 13$, $p = 0.805$; $t_{dark} = 1.370$, $df = 13$, $p = 0.194$) (Table 1). This is comparable to the pattern of effects in the LO, DLO, AIv and AId (see above). The distribution of cellular labelling intensities is strongly skewed to the right after play. Lightly stained neurons are lost and partly distributed over the medium as dark categories.

In summary, social play behaviour induced c-Fos expression in dorsal and ventral striatal regions. The c-Fos activation was most evident in the dorsal striatum, where more cells were present in all three intensity categories, indicative of a new population of cells that is recruited by

social play behaviour. The most pronounced changes in the ventral striatum were observed in the lCore and mShell, where social play increased the cell density of medium and dark cells.

It has been proposed that the classical division of the striatum into a dorsal and ventral part may not be the most appropriate functional division (Voorn et al. 2004). Therefore, we also analysed cellular activity in the striatum based on its inputs from the prefrontal cortex (Fig. 1c). This division revealed a gradient in the enhancement of the FpCD by social play. The largest increase was observed in the dorsolateral striatum, which corresponds to the part receiving input from the sensory and motor cortex (STR-SomSen = 9.463, $df = 13$, $p < 0.001$) (Fig. 8a). The magnitude of the increase in the FpCD was less prominent in the central and medial dorsal striatum. Significant increases in the FpCD were observed in the AC projection region (STR-AC: $t = 5.509$, $df = 13$, $p < 0.001$). In the projection area of the PrLd (STR-PrLd) a trend towards an increase was observed ($t = 1.786$, $df = 13$, $p = 0.097$), while in the PrLv projection area (STR-PrLv) a significant increase in the FpCD was seen ($t = 2.239$, $df = 13$, $p = 0.043$) (Fig. 8a). In the projection areas located in the ventral striatum, no changes in the FpCD were observed [IL projection area (STR-IL): $t = 0.400$, $df = 13$, $p = 0.696$; AId projection area (STR-AId): $t = 0.870$, $df = 13$, $p = 0.400$; AIv projection area (STR-AIv): $t = 0.218$, $df = 13$, $p = 0.831$] (Fig. 8a).

FpCD was also analysed in the striatum based on its inputs from the OFC (Groenewegen and Uylings 2010) (Fig. 1d). The striatal target regions of the OFC projections partially overlap with those from the mPFC. Indeed, a comparable gradient of c-Fos activation was observed
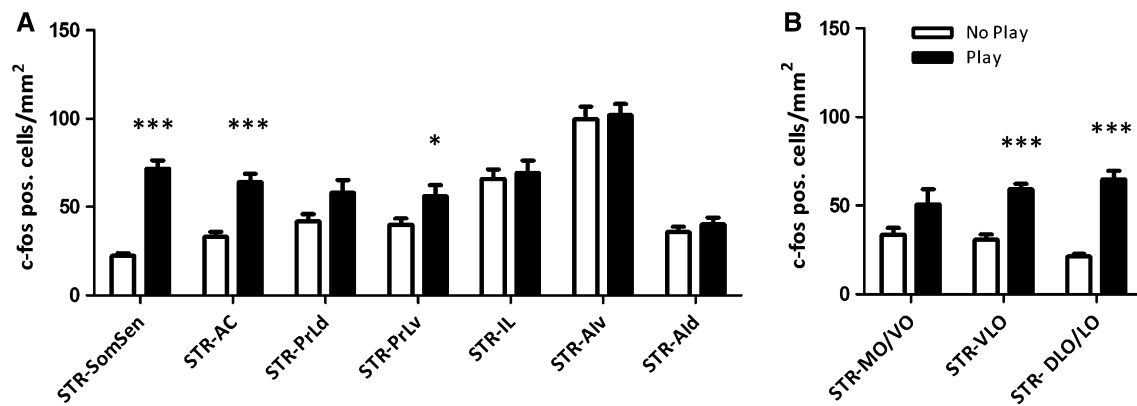
Fig. 8 The c-Fos activity induced by social play behaviour in the striatum shows a dorsolateral to ventromedial gradient. The c-Fos-positive cell density was determined in rats after receiving a play session ('play' group) and in rats that were placed in the test cage without a partner present ('no-play' group). The striatum was divided according to mPFC inputs (**a**) and OFC inputs (**b**). Data are presented as mean ± SEM. *$p < 0.05$, ***$p < 0.001$, different from the no-play group. *STR-* striatal region receiving input from cortical region, *SomSen* somatosensory cortex, *AC* anterior cingulate cortex, *PrLd* prelimbic cortex dorsal part, *PrLv* prelimbic cortex ventral part, *IL* infralimbic cortex, *AIv* agranular insular cortex ventral part, *AId* agranular insular cortex dorsal part, *MO/VO* medial/ventral orbito-frontal cortex, *VLO* ventrolateral orbitofrontal cortex, *DLO/LO* dorsolateral/lateral orbitofrontal cortex

(Fig. 8b). A large increase was observed in the dorsolateral striatum region receiving inputs from the DLO and LO (STR-DLO/LO: $t = 8.143$, $df = 13$, $p < 0.001$). The central part of the striatum receives inputs from the VLO, where an increase in the FpCD was also observed (STR-VLO: $t = 6.414$, $df = 13$, $p < 0.001$). In the medial part of the striatum, receiving input from the MO and VO, no effects of play were detected (STR-MO/VO: $t = 1.728$, $df = 13$, $p = 0.108$).

In these different divisions of the striatum, the FpCD was also analysed based on intensity of the cells (Table 1). In the dorsolateral striatal parts characterized by cortical inputs from sensori-motor and orbitofrontal (DLO/LO) regions, an increase in the FpCD was observed in all categories (STR-SomSen: $F_{play \times category}(2,39) = 29.351$, $p < 0.001$; $t_{light} = 4.201$, $df = 13$, $p = 0.001$; $t_{medium} = 8.711$, $df = 13$, $p < 0.001$; $t_{dark} = 8.697$, $df = 7.409$, $p < 0.001$; STR-DLO/LO: $F_{play \times category}(2,39) = 27.009$, $p < 0.001$; $t_{light} = 2.393$, $df = 13$, $p = 0.033$; $t_{medium} = 7.099$, $df = 13$, $p < 0.001$; $t_{dark} = 8.698$, $df = 7.594$, $p < 0.001$). This clearly suggests a rightward and upward shift of the OD distribution, with the highest increases in the dark cell categories. Both cellular response rate and the number of reactive cells are increased after social play, probably through recruitment of a newly reactive population of cells.

A response pattern indicating primarily a rightward shift in the population distribution and more cells reaching the detection limit, was found in the striatal regions targeted by AC and VLO, and to a lesser extent the regions reached by inputs from PrLd and PrLv (Table 1). Proportionally large increases were observed in the dark and medium cell classes of STR-AC, but changes were absent in the lightly stained cellular category ($F_{play \times category}(2,39) = 10.476$, $p < 0.001$; $t_{light} = 0.843$, $df = 13$, $p = 0.415$; $t_{medium} = 6.255$, $df = 13$, $p < 0.001$; $t_{dark} = 5.248$, $df = 8.654$, $p = 0.001$). Similar results were obtained for STR-VLO ($F_{play \times category}(2,39) = 7.771$, $p = 0.001$; $t_{light} = 1.614$, $df = 13$, $p = 0.130$; $t_{medium} = 5.909$, $df = 13$, $p < 0.001$; $t_{dark} = 5.193$, $df = 9.465$, $p < 0.001$). In the striatum regions receiving input from the PrLd and PrLv, social play behaviour enhanced the FpCD only in the dark category (STR-PrLd: $F_{play \times category}(2,39) = 3.776$, $p = 0.032$; $t_{light} = -1.251$, $df = 13$, $p = 0.233$; $t_{medium} = 1.625$, $df = 13$, $p = 0.128$; $t_{dark} = 2.239$, $df = 13$, $p = 0.043$; STR-PrLv: $F_{play \times category}(2,39) = 4.878$, $p = 0.013$; $t_{light} = -1.548$, $df = 13$, $p = 0.146$; $t_{medium} = 2.157$, $df = 13$, $p = 0.050$; $t_{dark} = 2.578$, $df = 9.252$, $p = 0.029$). STR-MO/VO shows the same tendencies, albeit that differences were not significant ($F_{play \times category}(2,39) = 2.979$, $p = 0.063$).

In the STR-IL, STR-AIv and STR-AId sectors, a decrease in FpCD was detected in the light category, with changes in STR-AId being not significant (STR-IL: $F_{play \times category}(2,39) = 4.920$, $p = 0.012$; $t_{light} = -2.605$, $df = 13$, $p = 0.022$; $t_{medium} = -0.064$, $df = 13$, $p = 0.950$; $t_{dark} = 1.965$, $df = 13$, $p = 0.071$; STR-AIv: $F_{play \times category}(2,39) = 3.820$, $p = 0.031$; $t_{light} = -3.099$, $df = 13$, $p = 0.008$; $t_{medium} = 0.300$, $df = 13$, $p = 0.769$; $t_{dark} = 1.414$, $df = 13$, $p = 0.181$; STR-AId: $F_{play \times category}(2,39) = 5.042$, $p = 0.011$; $t_{light} = -1.830$, $df = 13$, $p = 0.090$; $t_{medium} = 1.134$, $df = 13$, $p = 0.277$; $t_{dark} = 2.162$, $df = 13$, $p = 0.050$). Since overall FpCd—regardless of staining intensity—had not changed as a

consequence of play behaviour, it may be concluded that the response pattern in the above three striatal regions represents skewing to the right, i.e. the response intensity at the cellular level was enhanced. However, these changes were of moderate strength because they did not result in a significant increase in the dark or medium cellular compartments.

To summarize, social play behaviour increased the FpCD in different categories of the striatal regions: all categories in the dorsolateral striatum, medium and dark category in the central dorsal striatal region, dark category in the dorsomedial regions, and decreased the FpCD in the light category in the ventromedial striatal regions. This suggests that the recruitment of new cells by social play behaviour is most apparent in the dorsolateral striatum, an effect which tapers off in the medial and ventral direction. In these latter regions, it may also be that cells that were already active express more c-Fos after play. Together, these results indicate that the induction of c-Fos gene expression by social play behaviour is topographically organized within the striatum.
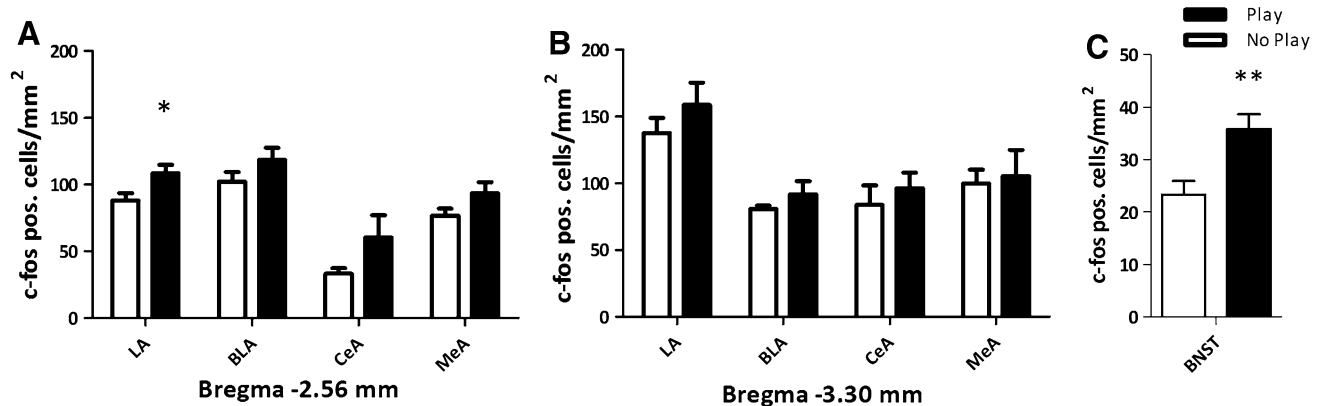
Amygdala

The FpCD was determined in several amygdala regions: the lateral amygdala (LA), basolateral amygdala (BLA), central amygdala (CeA), and medial amygdala (MeA). The FpCD was measured in these regions at 2 different anterior–posterior levels (-2.56 and -3.30 mm from Bregma; Fig. 1f, g). These two levels were chosen since initial visual inspection of c-Fos-positive staining in both groups suggested the presence of anterior–posterior differences. In addition, the FpCD was determined in a region of the

extended amygdala, the bed nucleus of the stria terminalis (BNST) (Fig. 1e).

Social play increased the FpCD in the LA at the anterior level ($t = 2.428$, $df = 14$, $p = 0.029$), but not at the posterior level ($t = 1.053$, $df = 14$, $p = 0.310$) (Fig. 9a, b). Social play increased the FpCD in the BNST ($t = 3.288$, $df = 14$, $t = 0.005$) (Fig. 9c). In the other subregions of the amygdala no effect on the FpCD was observed at either level ($t < 1.803$, $p > 0.092$) (Fig. 9a, b).

Division into the three categories showed that the effect in the anterior LA was due to an increase in medium and dark cells ($F_{\text{play}\times\text{category}}(2,42) = 5.77$, $p = 0.006$; $t_{\text{light}} = -1.728$, $df = 14$, $p = 0.1061$; $t_{\text{medium}} = 2.581$, $df = 14$, $p = 0.022$; $t_{\text{dark}} = 2.432$, $df = 14$, $p = 0.029$) (Table 1). In the anterior BLA an increase in FpCD was observed in the dark category ($F_{\text{play}\times\text{category}}(2,42) = 4.758$, $p = 0.014$; $t_{\text{light}} = -1.552$, $df = 14$, $p = 0.143$; $t_{\text{medium}} = 0.906$, $df = 14$, $p = 0.380$; $t_{\text{dark}} = 2.389$, $df = 14$, $p = 0.032$), while no effect was observed in the posterior BLA ($F_{\text{play}\times\text{category}}(2,42) = 2.158$, $p = 0.149$) (Table 1). In the other subregions, no alterations were detected in any of the intensity categories ($F_{\text{play}\times\text{category}} < 2.710$, $p > 0.077$).

In summary, social play increased the FpCD specifically in the anterior LA and BNST. In the LA, increases in the FpCD in the medium and dark category were observed, which may be the result of new cells being recruited by play, or a result of cells that were already active expressing more c-Fos. In the BNST, no significant interaction was observed between the effect of play and the different categories, probably indicating that a new population of cells was recruited by social play. In the anterior BLA no overall changes in FpCD were observed, but the FpCD was enhanced in the dark category. These results suggest that in

Fig. 9 Social play behaviour increased the c-Fos-positive cell density in the lateral amygdala and bed nucleus of the stria terminalis. The c-Fos-positive cell density was determined in rats after receiving a play session ('play' group) and in rats that were placed in the test cage without a partner present ('no-play' group). Regions measured include the lateral amygdala (LA), basolateral amygdala (BLA), central amygdala (CeA) and medial amygdala (MeA) at two different anterior posterior levels, -2.56 mm from Bregma (a) and -3.30 mm from Bregma (b) and the bed nucleus of the stria terminalis (BNST) (c). Data are presented as mean ± SEM. *$p < 0.05$, **$p < 0.01$, different from the no-play group
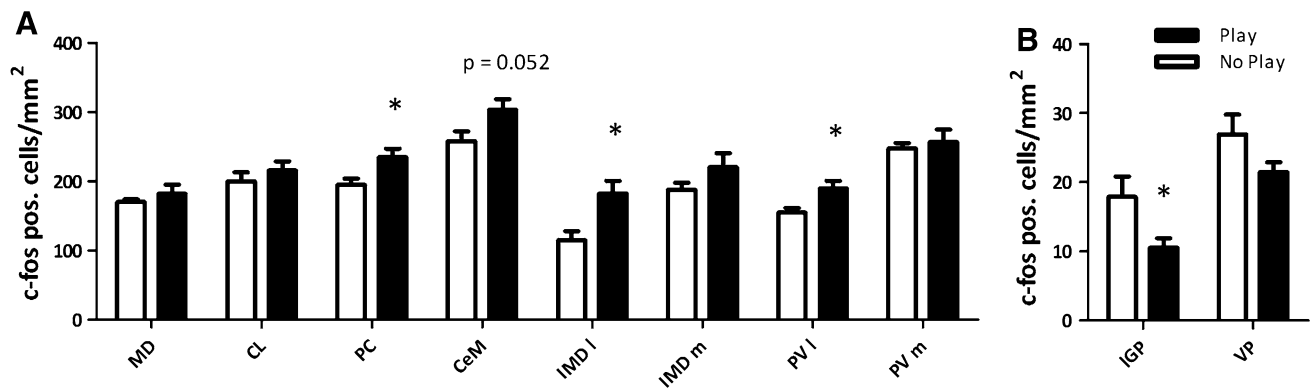
Fig. 10 Social play-induced changes in the c-Fos positive cell density in the thalamus and pallidum. The c-Fos-positive cell density was determined in rats after receiving a play session ('play' group) and in rats that were placed in the test cage without a partner present ('no-play' group). Social play behaviour increased c-Fos activity in several thalamic regions, while decreasing c-Fos activity in the lGP. The thalamic regions measured are presented in panel **a** and the pallidum regions are presented in panel **b**. Data are presented as mean ± SEM. *$p < 0.05$, different from the no-play group. *MD* mediodorsal thalamic nucleus, *CL* central lateral thalamic nucleus, *PC* paracentral thalamic nucleus, *CeM* central medial thalamic nucleus, *IMDl* intermediodorsal thalamic nucleus lateral part, *IMDm* intermediodorsal thalamic nucleus medial part, *PVl* paraventricular thalamic nucleus lateral part, *PVm* paraventricular thalamic nucleus medial part, *lGP* lateral globus pallidus, *VP* ventral pallidum

the BLA no new cells were recruited, but the same cells expressed more c-Fos after a play session.

Thalamus

Within the thalamus, we investigated regions highly connected to the striatum and prefrontal cortex; these included the mediodorsal thalamic nucleus (MD) and several of the midline and intralaminar thalamic nuclei: the central lateral thalamic nucleus (CL), the paracentral thalamic nucleus (PC), the central medial thalamic nucleus (CeM), the medial and lateral parts of the intermediodorsal thalamic nucleus (IMDm and IMDl), and the medial and lateral paraventricular thalamic nucleus (PVm and PVl) (Fig. 1f).

Social play behaviour increased the FpCD in the PC ($t = 2.642$, $df = 13$, $p = 0.020$), the IMDl ($t = 2.993$, $df = 14$, $p = 0.010$) and in the PVl ($t = 2.689$, $df = 13$, $p = 0.019$) (Fig. 10a). A trend towards an increase was observed in the CeM ($t = 2.125$, $df = 14$, $p = 0.052$), while in the other thalamic regions no differences in the FpCD were detected ($t < 1.421$, $p > 0.177$) (Fig. 10a). Division of the cells into three categories showed a trend towards an interaction between intensity category and the effect of play in the IMDl ($F_{play \times category}(2,42) = 3.026$, $p = 0.059$), while no effects were observed in any of the other regions ($F_{play \times category} < 1.830$, $p > 0.173$) (Table 1).

To summarize, these data indicate that social play induced c-Fos expression in several thalamic regions, including the PC, IMDl, and PVl. The enhancement of the FpCD in these regions was equally distributed over the different intensity categories, suggesting that a new population of cells was recruited by social play in these regions.

Pallidum

The FpCD was determined in the lateral globus pallidus (lGP) and ventral pallidum (VP) (Fig. 1e). The FpCD was decreased in the play group in the lGP ($t = -2.277$, $df = 14$, $p = 0.039$) (Fig. 10b). This was not due to a specific effect in any of the expression level categories, since there was no interaction with the effect of play ($F_{play \times category}(2,42) = 1.202$, $p = 0.311$) (Table 1). In the ventral pallidum no differences were observed on the overall FpCD, nor was there an interaction with the different expression levels categories ($t = -1.740$, $df = 14$, $p = 0.104$; $F_{play \times category}(2,42) = 0.110$, $p = 0.896$) (Fig. 10b; Table 1). These results indicate that social play behaviour decreases c-Fos expression in the lGP which is equally distributed over the different intensity categories. This is indicative of a population of cells that is inhibited during play behaviour in the lGP.

Monoamine nuclei

c-Fos expression levels after social play were also analysed in monoamine nuclei, such as the ventral tegmental area (VTA), substantia nigra pars compacta (SNc), locus coeruleus (LC), and the dorsal raphe nucleus at two different levels (DRa at −8.00 mm from Bregma, DRp at −8.72 mm from Bregma), as well as the substantia nigra pars reticulata (SNr) (Fig. 1h, j–l). No changes were observed in the VTA ($t = -0.236$, $df = 14$, $p = 0.817$), SNc ($t = -0.207$, $df = 14$, $p = 0.839$) and SNr ($t = -0.089$, $df = 14$, $p = 0.930$) (Fig. 11a). In the dorsal raphe an increase in the FpCD was detected at the anterior level ($t = 2.637$, $df = 13$, $p = 0.021$), while no alterations
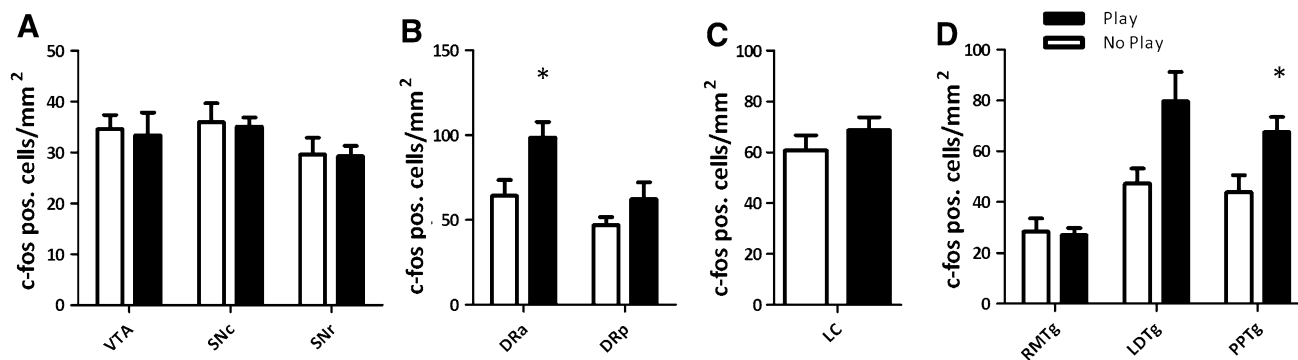
Fig. 11 Social play-induced changes in monoamine nuclei and tegmental regions. The c-Fos-positive cell density was determined in rats after receiving a play session ('play' group) and in rats that were placed in the test cage without a partner present ('no-play' group). After a social play session the level of c-Fos activity was increased in the anterior dorsal raphe nucleus and the PPTg relative to the 'no-play' control. Regions measured included the ventral tegmental area (*VTA*), substantia nigra pars compacta (*SNc*) and substantia nigra pars reticulata (*SNr*) (**a**), dorsal raphe nucleus anterior and posterior level (*DRa* and *DRp*, **b**), locus coeruleus (*LC*, **c**), rostromedial tegmental nucleus (*RMTg*), laterodorsal tegmental nucleus (*LDTg*), and pedunculopontine tegmental nucleus (*PPTg*) (**d**). Data are presented as mean ± SEM. *$p < 0.05$, different from the no-play group

were observed in the DR at the posterior level ($t = 1.446$, $df = 14$, $p = 0.170$) (Fig. 11b). No changes were observed in the LC after social play ($t = 0.994$, $df = 13$, $p = 0.338$) (Fig. 11c). No interactions were observed between play and the different categories of c-Fos expression levels in any of these regions ($F_{play \times category}$ $t < 2.757$, $p > 0.075$) (Table 1). These results suggest that social play behaviour did not induce c-Fos expression in the dopamine- and noradrenaline-producing regions, while it did affect c-Fos expression in the serotonin-producing dorsal raphe nucleus. Since the increase in the FpCD was equally distributed over the different intensity categories, it is likely that in the anterior DR a new population of cells was recruited by social play behaviour.

Rostromedial tegmental nucleus, laterodorsal tegmental nucleus and pedunculopontine tegmental nucleus

Expression levels of c-Fos, induced by play, were analysed in the rostromedial tegmental nucleus (RMTg), the laterodorsal tegmental nucleus (LDTg) and pedunculopontine tegmental nucleus (PPTg) (Fig. 1i–k). Social play increased the FpCD in the PPTg ($t = 2.642$, $df = 14$, $p = 0.019$), but not in RMTg or LDTg (RMTg: $t = -0.233$, $df = 14$, $p = 0.819$; LDTg: $t = 0.683$, $df = 14$, $p = 0.506$) (Fig. 11d). However, when taking into account the intensity level and comparing the FpCD per category, there was an increase in the dark cells in the RMTg ($F_{play \times category}(2,40) = 4.877$, $p = 0.013$; $t_{light} = -1.935$, $df = 14$, $p = 0.073$; $t_{medium} = -0.112$, $df = 14$, $p = 0.913$; $t_{dark} = 2.665$, $df = 14$, $p = 0.018$), suggesting that the same population of neurons expressed more c-Fos after play. In the other regions no interaction between play

and the FpCD in the three categories was observed ($F_{play \times category}$ $t < 0.263$, $p > 0.770$) (Table 1).

In summary, these results suggest that in the RMTg the same population of neurons expressed more c-Fos after social play behaviour, while in the PPTg a new population of cells is recruited.

Correlations in social play-induced c-Fos activity

To gain insight in the neural network activated during social play behaviour, correlations of c-Fos activity were assessed between regions with known anatomical interconnections. The focus of this analysis was on connections of the prefrontal cortex and striatum with each other as well as with the amygdala, thalamus and VTA/SN complex.

Correlations of c-Fos immunoreactivity between the prefrontal, striatal and thalamus regions were investigated because the three brain regions are strongly interconnected in a topographical manner (Groenewegen and Uylings 2010; Schilman et al. 2008; Van der Werf et al. 2002; Voorn et al. 2004). The same holds for the relationship between amygdala, prefrontal cortex and striatum. The BLA provides most inputs to the striatum (Kelley et al. 1982; Voorn et al. 2004), while all nuclei (measured as regions of interest in the present study) provide inputs and receive outputs from the prefrontal cortex (Cassell and Wright 1986; McDonald et al. 1996; Voorn et al. 2004). For this reason, correlations between BLA and striatum as well as correlations between all amygdala regions and prefrontal regions were analysed.

The VTA and SN have reciprocal projections with the striatum and prefrontal cortex, where the VTA and SNc provide a dopaminergic projection to both regions and the

VTA, SNc and SNr receive GABAergic outputs from the striatum (Gerfen et al. 1987; Gerfen 2004; Ikemoto 2007; Watabe-Uchida et al. 2012). Correlations of the VTA and SNc with the prefrontal and striatal regions were analysed, as well as correlations between the SNr and striatal regions.

An overview of all correlations analysed is presented in Table 2. In addition, a summary of these correlations is visualized in a network figure, which indicates the substantial differences between the 'play' and 'no-play' groups that are described below (Fig. 12).

Prefrontal cortex correlations

Significant correlations were observed between the striatal target regions and the cortical input regions in the projections of the mPFC regions PrLd, PrLv, and IL, and agranular insular regions, AId and AIv, in the play group (Table 2), whereas such correlations were absent in the no-play group. In addition, no correlations were detected in play or no-play animals in the OFC projections to the striatum, or between the thalamus regions and their mPFC projection areas (Table 2). Activity in the IMDl region of the thalamus did correlate with the AIv in the play group, while not correlating in the no-play group (Table 2).

c-Fos immunoreactivity levels in the BLA and MEA subnuclei of the amygdala correlated with several prefrontal cortex regions in the play group (Table 2). Correlations were observed between the anterior BLA and all mPFC regions, the ventral and lateral OFC regions, and the agranular insular cortex. These correlations were only present in the play group. At the posterior level correlations between the BLA and prefrontal regions were less pronounced, being significant in PrL, IL and AId in the play group, and in LO in the no-play group (Table 2). Activity in the anterior MeA correlated with the c-Fos activity in the PrL, IL, VO, VLO, AId, and AIv and these correlations were specific for the play group. Comparable to the BLA, activity in the posterior MeA correlated with activity in fewer prefrontal regions (i.e. PrL and DLO only) relative to the anterior MeA. No correlations were observed between the prefrontal regions and the anterior LA or anterior CeA, while with the posterior LA and CeA a few correlations were observed (IL, VO and MO, VO, respectively) (Table 2).

Correlations were observed between the VTA and all mPFC regions as well as with the VLO, specifically in the play group. The c-Fos activity in the SNc correlated negatively with the activity in the AC and LO, also in the play group only (Table 2).

In summary, in playing animals the most pronounced correlations in prefrontal cortex regions were observed between mPFC and striatum, between prefrontal cortex and BLA as well as MeA, and between the mPFC and VTA (Fig. 12).

Striatum correlations

For most thalamus regions, no correlations were observed in the c-Fos immunoreactivity levels with those measured in their striatal projection regions, except for the PVm and its striatal target area. This correlation was specific for the play group (Table 2).

The c-Fos immunoreactivity levels in the anterior BLA correlated with the levels measured in several ventral striatum regions, i.e. the mCore, mShell, lShell, and OTu, specifically in the play group. A comparable pattern of correlations was observed for the posterior BLA, except that at this level activity in the lShell did not correlate, while activity in the vShell did correlate with activity in the posterior BLA (Table 2).

The c-Fos immunoreactivity levels in the VTA correlated only with the c-Fos levels observed in the most ventral regions of the striatum: mShell, vShell, and OTu. These correlations were specific for the play group. In contrast, the c-Fos levels in the SNc did not correlate with the levels in any of the striatal regions. c-Fos immunoreactivity levels did correlate between the SNr and the mCore in the play group. In addition, the activity levels of the SNr correlated with the levels measured in the lCore in the no-play animals (Table 2).

The social play-induced c-Fos levels in the VP correlated with those in the mShell and lShell in the play group. In addition, c-Fos immunoreactivity levels in the VP and lGP correlated negatively with the levels in the lCore in the no-play group (Table 2).

In summary, in the striatum of the playing animals the most pronounced correlations of the c-Fos immunoreactivity levels were observed between BLA and ventral striatal regions, between VTA and NaShell as well as OTu and between NaShell and VP (Fig. 12).

Discussion

In the present study, social play-induced c-Fos activity was measured to investigate the neural substrates of this behaviour. The induction of c-Fos expression is widely used as a neuronal activity marker (Kovacs 2008; Morgan and Curran 1991; Schilling et al. 1991), since neurotransmitter receptor activation, depolarization, and growth factors are known to induce c-Fos expression. Therefore, increases in c-Fos expression levels can be interpreted as a cellular response to the given stimulus in these cells. However, it remains important to keep in mind that neuronal activation can occur in the absence of c-Fos induction

Table 2 Overview of correlations

Reg. 1	Reg. 2	Play Cor.C	p val.	No play Cor.C	P val.	Reg. 1	Reg. 2	Play Cor.C	p val.	No play Cor.C	p val.
Prefrontal–striatum						*Amygdala (−2.56 mm)–prefrontal (continued)*					
AC	STR-AC	0.357	0.432	0.464	0.294	LA	IL	−0.257	0.623	−0.086	0.872
PrLd	STR-PrLd	**0.738**	**0.037**	0.214	0.645	LA	MO	−0.290	0.957	−0.029	0.957
PrLv	STR-PrLv	**0.952**	**<0.001**	0.357	0.432	LA	VO	−0.486	0.329	−0.086	0.872
IL	STR-IL	**0.857**	**0.014**	−0.071	0.879	LA	VLO	−0.429	0.397	0.543	0.260
MO	STR-MO/VO	0.536	0.215	−0.071	0.879	LA	LO	−0.486	0.329	0.771	0.072
VO	STR-MO/VO	0.464	0.294	0.607	0.148	LA	DLO	−0.086	0.872	0.314	0.544
VLO	STR-VLO	0.321	0.482	−0.107	0.819	LA	AId	<0.001	>0.999	−0.314	0.544
LO	STR-LO/DLO	−0.214	0.645	−0.536	0.215	LA	AIv	−0.071	0.879	0.657	0.156
DLO	STR-LO/DLO	−0.486	0.329	0.036	0.939	CeA	AC	0.429	0.937	−0.771	0.072
AId	STR-AId	**0.881**	**0.004**	0.107	0.819	CeA	PrL	0.200	0.704	−0.314	0.544
AIv	STR-AIv	**0.881**	**0.004**	0.714	0.071	CeA	IL	−0.257	0.623	−0.771	0.072
Thalamus–striatum						CeA	MO	−0.314	0.544	−0.600	0.208
CL	STR-SomSen	−0.357	0.879	−0.771	0.072	CeA	VO	−0.371	0.468	−0.600	0.208
PC	STR-AC	−0.086	0.872	−0.086	0.872	CeA	VLO	0.257	0.623	0.371	0.468
CeM	STR-PrLd	0.607	0.148	−0.200	0.704	CeA	LO	0.657	0.156	0.714	0.111
PVm	STR-PrLv	**0.785**	**0.036**	0.314	0.544	CeA	DLO	0.257	0.623	0.714	0.111
PVl	STR-IL	−0.321	0.482	0.314	0.544	CeA	AId	<0.001	>0.999	−0.257	0.623
IMDl	STR-AIv	0.750	0.052	−0.086	0.872	CeA	AIv	0.214	0.645	0.429	0.397
IMDm	STR-AId	0.679	0.094	−0.428	0.397	MeA	AC	0.714	0.111	0.029	0.957
Thalamus–prefrontal						MeA	PrL	**0.943**	**0.005**	−0.029	0.957
PC	AC	0.400	0.504	0.143	0.787	MeA	IL	**0.943**	**0.005**	0.029	0.957
CeM	PrLd	0.771	0.072	0.086	0.871	MeA	MO	0.771	0.072	−0.143	0.787
PVm	PrLv	0.600	0.208	0.429	0.397	MeA	VO	**0.829**	**0.042**	0.029	0.957
PVl	IL	−0.429	0.397	0.543	0.266	MeA	VLO	**0.886**	**0.019**	0.771	0.072
IMDl	AIv	**0.786**	**0.036**	0.429	0.397	MeA	LO	0.600	0.208	0.543	0.266
IMDm	AId	0.642	0.119	−0.657	0.156	MeA	DLO	0.771	0.072	0.086	0.872
Amygdala (−2.56 mm)–striatum						MeA	AId	**0.821**	**0.023**	−0.086	0.872
BLA	DS	0.036	0.939	−0.543	0.266	MeA	AIv	**0.929**	**0.003**	0.543	0.266
BLA	mCore	**0.821**	**0.023**	−0.371	0.468	*Amygdala (−3.30 mm)–prefrontal*					
BLA	lCore	0.393	0.383	−0.771	0.072	BLA	AC	0.771	0.072	−0.086	0.872
BLA	mShell	**0.821**	**0.023**	−0.371	0.468	BLA	PrL	**0.943**	**0.005**	−0.086	0.872
BLA	vShell	0.536	0.215	−0.143	0.787	BLA	IL	**0.943**	**0.005**	−0.086	0.872
BLA	lShell	**0.821**	**0.023**	0.486	0.329	BLA	MO	0.771	0.072	0.086	0.872
BLA	OTu	**0.786**	**0.036**	0.200	0.704	BLA	VO	0.600	0.208	0.086	0.872

Table 2 continued

Reg. 1	Reg. 2	Play Cor.C	Play p val.	No play Cor.C	No play P val.	Reg. 1	Reg. 2	Play Cor.C	Play p val.	No play Cor.C	No play p val.
Amygdala (−3.30 mm)−striatum						BLA	VLO	0.886	0.019	0.771	0.072
BLA	DS	0.107	0.819	−0.371	0.468	BLA	LO	0.657	0.156	**0.886**	**0.019**
BLA	mCore	**0.821**	**0.023**	0.143	0.787	BLA	DLO	0.714	0.111	0.086	0.872
BLA	lCore	0.321	0.482	−0.657	0.156	BLA	AId	**0.857**	**0.014**	−0.426	0.397
BLA	mShell	**0.964**	**<0.001**	0.143	0.787	BLA	AIv	0.714	0.071	0.771	0.072
BLA	vShell	**0.893**	**0.007**	0.371	0.468	LA	AC	0.257	0.623	0.029	0.957
BLA	lShell	0.464	0.294	−0.029	0.957	LA	PrL	0.600	0.208	0.029	0.957
BLA	OTu	0.679	0.093	0.600	0.208	LA	IL	**0.829**	**0.042**	0.029	0.957
Amygdala (−2.56 mm)−prefrontal						LA	MO	0.543	0.266	−0.257	0.623
BLA	AC	**0.943**	**0.005**	0.715	0.111	LA	VO	**0.943**	**0.005**	0.543	0.266
BLA	PrL	**0.943**	**0.005**	−0.600	0.208	LA	VLO	0.543	0.266	0.714	0.111
BLA	IL	**0.829**	**0.042**	−0.714	0.111	LA	LO	0.143	0.787	0.257	0.623
BLA	MO	0.543	0.266	−0.086	0.872	LA	DLO	0.714	0.111	0.143	0.787
BLA	VO	0.600	0.208	−0.371	0.468	LA	AId	0.679	0.094	0.543	0.266
BLA	VLO	**>0.999**	**<0.001**	0.257	0.623	LA	AIv	0.714	0.071	0.771	0.072
BLA	LO	**0.886**	**0.019**	0.714	0.111	CeA	AC	−0.086	0.872	−0.314	0.544
BLA	DLO	**0.943**	**0.005**	0.143	0.787	CeA	PrL	−0.486	0.329	−0.029	0.957
BLA	AId	**0.893**	**0.007**	−0.714	0.111	CeA	IL	−0.771	0.072	−0.314	0.544
BLA	AIv	**>0.999**	**<0.001**	0.257	0.623	CeA	MO	−0.657	0.156	**−0.829**	**0.042**
LA	AC	−0.257	0.623	−0.086	0.872	CeA	VO	**−0.886**	**0.019**	**−0.829**	**0.042**
LA	PrL	−0.543	0.266	0.314	0.544	CeA	VLO	−0.371	0.468	0.086	0.872

(Kovacs 2008). In addition, induction of c-Fos may not be detected in chronically activated neurons (Kovacs 2008; Morgan and Curran 1991; Schilling et al. 1991).

Social play behaviour altered c-Fos expression in several of the measured brain regions. These alterations were observed in regions involved in reward processing and motivation, as well as in regions important for processing of motor and sensory information. During play behaviour, rats exhibit high levels of locomotor activity and process a large amount of sensory information (Gordon et al. 2002; Pellis and Pellis 1998; Vanderschuren et al. 1997). This kind of locomotor activity and sensory processing did not occur in the control rats, since they were alone in the test cage. Behaviour expressed by the control rats existed mainly of exploration and self-grooming. Therefore, in this study all sensory, emotional

and behavioural aspects of social play behaviour contributed to the observed effects. Note that, even though the animals in the play group spent a substantial amount of time on social play during testing, we cannot exclude that non-playful (social or non-social) activities contributed to the changes in c-Fos expression. Future studies will need to elucidate the neural underpinnings of the separate component processes that constitute social play, and whether the effect of some of these component processes (e.g. vigorous motor activity) on c-Fos expression is specific for social play.

Prefrontal cortex

Several prefrontal regions were activated as a result of social play behaviour. The largest increases in the FpCD

Table 2 continued

		Play		No play				Play		No play	
Reg. 1	Reg. 2	Cor.C	p val.	Cor.C	P val.	Reg. 1	Reg. 2	Cor.C	p val.	Cor.C	p val.
Amygdala (−3.30 mm)–prefrontal (continued)						*VTA/SN–prefrontal*					
CeA	LO	0.086	0.872	0.029	0.957	VTA	AC	**0.829**	**0.042**	−0.543	0.266
CeA	DLO	0.371	0.468	0.771	0.072	VTA	PrL	**0.886**	**0.019**	−0.600	0.208
CeA	AId	0.071	0.879	0.270	0.623	VTA	IL	**0.886**	**0.019**	−0.543	0.266
CeA	AIv	0.143	0.760	−0.143	0.787	VTA	MO	0.600	0.208	−0.143	0.787
MeA	AC	0.600	0.208	0.086	0.872	VTA	VO	0.771	0.072	0.314	0.544
MeA	PrL	**0.829**	**0.042**	−0.200	0.704	VTA	VLO	**0.943**	**0.005**	−0.486	0.329
MeA	IL	0.600	0.208	0.086	0.872	VTA	LO	0.714	0.111	−0.429	0.397
MeA	MO	0.314	0.544	−0.086	0.872	VTA	DLO	0.700	0.188	−0.029	0.957
MeA	VO	0.714	0.111	0.600	0.208	VTA	AId	0.679	0.094	0.371	0.468
MeA	VLO	0.771	0.072	−0.200	0.704	VTA	AIv	0.607	0.148	−0.143	0.787
MeA	LO	0.714	0.111	−0.657	0.156	SNc	AC	**−0.829**	**0.042**	−0.657	0.156
MeA	DLO	**0.829**	**0.042**	−0.200	0.704	SNc	PrL	−0.657	0.156	−0.714	0.111
MeA	AId	0.500	0.253	0.771	0.072	SNc	IL	−0.371	0.468	−0.657	0.156
MeA	AIv	0.714	0.071	−0.086	0.872	SNc	MO	−0.029	0.957	−0.486	0.329
VTA/SN–striatum						SNc	VO	−0.143	0.787	−0.143	0.787
VTA	DS	<0.001	>0.999	0.371	0.468	SNc	LO	**−0.943**	**0.005**	0.200	0.704
VTA	mCore	0.679	0.094	0.086	0.872	SNc	DLO	−0.800	0.104	0.257	0.623
VTA	lCore	0.143	0.760	0.429	0.397	SNc	AId	−0.607	0.148	0.086	0.872
VTA	mShell	**0.786**	**0.036**	0.086	0.872	SNc	AIv	−0.714	0.071	0.200	0.704
VTA	vShell	**0.821**	**0.023**	−0.086	0.872					*Pallidum–striatum*	
VTA	lShell	0.286	0.535	0.486	0.329	VP	DS	0.214	0.645	−0.771	0.072
VTA	OTu	**0.821**	**0.023**	0.029	0.957	VP	mCore	0.679	0.094	−0.600	0.208
SNc	DS	−0.500	0.253	0.371	0.468	VP	lCore	0.500	0.253	**−0.886**	**0.019**
SNc	mCore	−0.357	0.432	0.314	0.544	VP	mShell	**0.857**	**0.014**	−0.600	0.208
SNc	lCore	−0.286	0.535	−0.086	0.872	VP	vShell	0.536	0.215	−0.600	0.208
SNc	mShell	−0.571	0.180	0.314	0.544	VP	lShell	**0.786**	**0.036**	−0.086	0.872
SNc	vShell	−0.643	0.119	0.371	0.468	VP	OTu	0.679	0.094	−0.143	0.787
SNc	lShell	−0.571	0.180	0.771	0.072	lGP	DS	−0.250	0.589	−0.714	0.111
SNc	OTu	−0.393	0.383	0.429	0.397	lGP	mCore	0.179	0.702	−0.429	0.397
SNr	DS	−0.464	0.294	0.600	0.208	lGP	lCore	-0.286	0.535	**−0.943**	**0.005**
SNr	mCore	**0.929**	**0.003**	0.086	0.872	lGP	mShell	0.179	0.702	−0.429	0.397
SNr	lCore	0.214	0.645	**0.943**	**0.005**	lGP	vShell	0.000	1.000	−0.429	0.397
SNr	mShell	0.750	0.052	0.086	0.872	lGP	lShell	0.357	0.432	0.029	0.957
SNr	vShell	0.429	0.337	0.086	0.872	lGP	OTu	0.429	0.337	0.143	0.787
SNr	lShell	0.357	0.432	0.257	0.623						
SNr	OTu	0.643	0.119	−0.429	0.397						

Correlations were determined in the 'Play' and 'No play' group for relevant projections. Significant correlations are presented in bold

Cor.C Spearman's rho correlation coefficient, *p val.* p value of this correlation coefficient
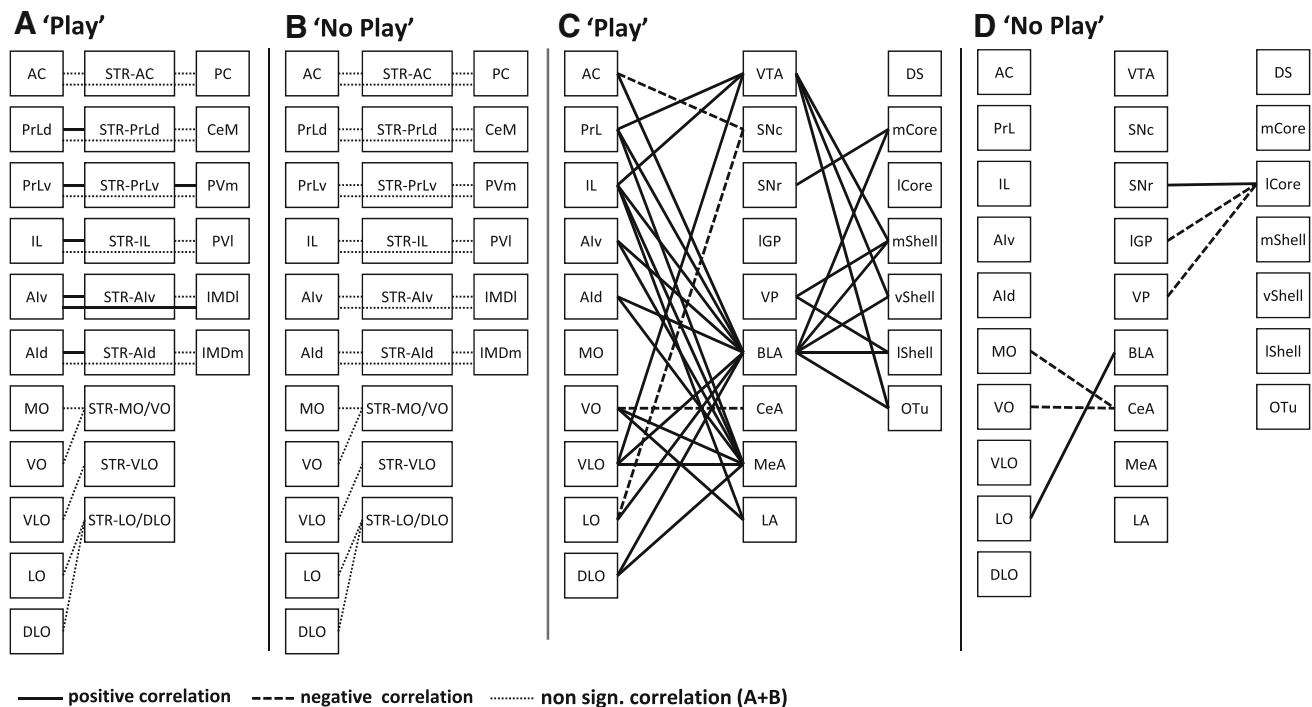
Fig. 12 Summary of correlations observed in 'play' and 'no-play' animals. Data are abstracted from Table 2 and represents Spearman's rho correlation coefficient. **a, b** Correlations in the thalamocortico-striatal network. Each region was only correlated with its known direct connections. *Black line* indicates a significant positive correlation, a *dotted line* indicates the absence of a significant correlation in the play (**a**) and no-play (**b**) groups. **c, d** Correlations of the amygdala, VTA and pallidum regions with the prefrontal cortex and striatum. *Black line* indicates a significant positive correlation, whereas the *dotted line* indicates a significant negative correlation in the play (**c**) and no-play (**d**) groups

were observed in the dorsal mPFC regions and medial OFC regions, while in the lateral OFC regions a reduction in the FpCD was observed. In the dorsal mPFC regions and medial OFC regions, the observed increase in number of c-Fos expressing cells upon play behaviour was caused by activation of a new population of cells in combination with higher levels of c-Fos expression in cells that were already active. In the IL and VO, the overall FpCD was not altered by social play behaviour, although more cells were present in the dark category suggesting that active cells express more c-Fos after social play behaviour in these regions.

Social play behaviour thus induced a heterogeneous activity pattern in the mPFC and OFC, suggesting that the various prefrontal subregions may have a different role in modulating social play behaviour. Neonatal lesion studies have previously implicated the mPFC and OFC in social play behaviour (Bell et al. 2009; Panksepp et al. 1994; Pellis et al. 1992, 2006; Schneider and Koch 2005). In addition, enhanced c-Fos activation after social play behaviour in rats has previously been reported in prefrontal regions (Gordon et al. 2002). Separate analysis of prefrontal subregions after play has been performed in golden hamsters (Cheng et al. 2008). Consistent with our study,

activation was observed in the AC, PrL, and IL, whereas the OFC was not investigated (Cheng et al. 2008).

Lesions of the mPFC and OFC have indicated dissociable roles of these regions in social play behaviour. Thus, neonatal lesions of the OFC did not alter the performance of play itself, but disrupted the partner-related modulation of play (Pellis et al. 2006). Adolescent rats respond in a distinct manner to dominant, subordinate and female rats, but animals with neonatal lesions of the OFC responded to all different partners alike (Pellis et al. 2006). Animals with neonatal lesions of the mPFC did show this partner-related change in social play behaviour. However, they expressed less complex defensive strategies compared to control rats (Bell et al. 2009).

In summary, it appears that the different prefrontal regions have distinct functions in relation to social play behaviour. Previously, different roles for the mPFC and OFC have been reported in the shaping of social play behaviour in relation to social cues (Bell et al. 2009; Pellis et al. 2006). The present study points towards heterogeneous functioning of the prefrontal regions in social play, which argues for future behavioural studies to include more detailed interventions in prefrontal function.

Corticostriatal systems

Similar to the prefrontal cortex, the different subregions of the striatum were not uniformly activated by social play behaviour. The largest increase in the FpCD was observed in the dorsolateral striatum, in all intensity categories, suggesting that a new population of cells was activated in this region. This activity may well be related to the high level of motor and sensory activity in the play group, since the dorsolateral striatum receives a great deal of sensori-motor information (Voorn et al. 2004). In addition, dopamine depletion in the striatum has been shown to result in alterations in the sequential order of play behaviour (Pellis et al. 1993), which is in line with an important role for the striatum in the processing of sensory and motor information, and the translation into behaviour during social play.

Although to a lesser extent, social play behaviour induced c-Fos activity in the ventral striatum as well, which confirms previous observations (Gordon et al. 2002). The increase in c-Fos activity in the ventral striatum was most pronounced in the lCore and mShell. Since these regions have been implicated in reward-related behaviours (Berridge and Kringelbach 2008; Cardinal et al. 2002; Haber and Knutson 2010; Kelley 2004; Nordquist et al. 2008; Sesack and Grace 2010; Voorn et al. 2004; Zahm 1999), the activity observed in the present experiments may be related to the rewarding properties of social play behaviour. Indeed, it has recently been reported that μ-opioid receptors in the NaCore and NaShell mediate the rewarding properties of social play behaviour (Trezza et al. 2011b).

Interestingly, in the play group, correlations were observed between c-Fos activity of the medial prefrontal/agranular insular regions and their striatal target regions. This is suggestive of a corticostriatal projection that is activated during social play behaviour. Previously, it has been reported that stimulation of cortical regions results in topographically organized induction of immediate early genes in the striatum (Miyachi et al. 2005; Parthasarathy and Graybiel 1997), which suggests that c-Fos activity in the striatum after play is in part caused by activity of the prefrontal cortex. At present, our understanding of the functional role of the parallel corticostriatal connections is limited. The projection from the mPFC to the dorsomedial striatum has previously been implicated in attention and goal-directed behaviour (Balleine et al. 2009; Christakou et al. 2001) and the mPFC to NaCore projection has been implicated in the integration of information about consequences of actions in relation to anticipated reward (Christakou et al. 2004), as well as in appetitive Pavlovian conditioning (Parkinson et al. 2000) and reinstatement of drug seeking (McFarland et al. 2003). Although these studies investigated the involvement of these projections in

a different type of behaviour, related processes may be involved during social play behaviour. Hypothetically, dorsal prefrontal-dorsomedial striatum projections may be involved in the sequential and temporal organization of play behaviour, whereas the ventral prefrontal-ventral striatum projections underlie the rewarding aspects of social play behaviour. Interestingly, lesions of the mPFC and depletion of dopamine in the striatum both resulted in the use of less complex defence strategies during play (Bell et al. 2009; Pellis et al. 1993), indicating that the generation of a playful defence strategy is indeed subserved by a corticostriatal projection.

In contrast to the mPFC and agranular insular cortex, no correlations were observed between the OFC and its striatal target regions, although social play-induced c-Fos activity was observed in the OFC. It cannot be excluded that the overlap in striatal projection areas of mPFC and OFC projections masked a correlation between OFC and striatal activity. As part of the c-Fos activity in the OFC projection regions may have been related to input from the mPFC, this may have overshadowed a correlation between activity in the OFC and striatal projection. Nevertheless, the correlation between mPFC and its striatal projection is apparently stronger than the possible correlation between OFC and striatum. Possibly, the OFC exerts its effects on play via different routes, with the amygdala as a potential candidate, since correlations were observed between OFC and amygdala regions (Table 2; Fig. 12). The OFC–amygdala connection is known to be involved in behavioural flexibility (Churchwell et al. 2009), and the encoding of the value of expected outcomes of actions (Schoenbaum et al. 2003), which may play a role in social play behaviour as well.

To conclude, cellular activity induced by social play behaviour is topographically organized in the corticostriatal system. The most pronounced alterations were observed in the dorsal mPFC, medial OFC, dorsal striatum, lCore and mShell. In addition, correlation analysis indicated a role for the mPFC-striatum and agranular insular cortex-striatum projections in social play behaviour.

Amygdala

Social play behaviour increased the expression of c-Fos in the anterior LA, anterior BLA, and the BNST, the latter of which has been put forward to be part of the extended amygdala (Alheid 2003), while in the MeA and CeA no increases in the FpCD were observed. In the anterior BLA, no overall changes in FpCD were observed, but the FpCD was enhanced in the dark cell intensity category. These results suggest that in the BLA no new cells were recruited, but that the same cells expressed more c-Fos after a play session. Of the amygdala nuclei, the BLA provides most

inputs to the striatum (Kelley et al. 1982; Voorn et al. 2004). Interestingly, the c-Fos activity in the BLA correlated only in the play group with the activity in most parts of the striatum, with the exception of the most dorsolateral regions, which hardly receive amygdaloid projections (Kelley et al. 1982). These results indicate a role for the amygdalo-striatal projections in social play behaviour. In addition, c-Fos activity in the BLA correlated with most regions of the mPFC, several of the OFC regions, and the agranular insular cortex, suggesting an involvement of the BLA-prefrontal cortex projections in social play behaviour as well.

In line with our findings, induction of c-Fos expression in the BNST has previously been reported after play in golden hamsters (Cheng et al. 2008). In contrast to the present study, in golden hamsters social play-induced c-Fos expression was also observed in the MeA (Cheng et al. 2008). Interestingly, in our study correlations were observed between the c-Fos activity in the MeA and several orbitofrontal regions, suggesting that in rats the MeA-cortical connections may indeed play a role in social play behaviour.

It is widely accepted that the amygdala is important for the processing of negative emotions (Maren and Quirk 2004; Morrison and Salzman 2010; Phelps and Ledoux 2005). Over the past years, it has become clear that the amygdala is important for the processing of positive emotions as well (Baxter and Murray 2002; Cardinal et al. 2002; Morrison and Salzman 2010). Since one of the key features of social play behaviour is its positive emotional value (Trezza et al. 2011a; Vanderschuren 2010), it is reasonable to assume that the amygdala is involved in the pleasurable properties of play behaviour. Indeed, the size of the amygdala has been correlated with play behaviour in nonhuman primates, with a larger amygdala size being associated with a higher percentage of time spent on social play behaviour (Lewis and Barton 2006). In addition, neonatal lesions of the amygdala have been reported to affect social play behaviour (Daenen et al. 2002; Meaney et al. 1981), although these effects may be sex-specific (Meaney et al. 1981). Furthermore, it has recently been shown that the BLA is the site of action where endocannabinoids modulate social play reward (Trezza et al. 2012). Enhanced levels of endocannabinoid activity were found to be associated with increased social play behaviour, and increased endocannabinoid neurotransmission within the BLA was necessary and sufficient for this enhancement of social play behaviour (Trezza et al. 2012).

Taken together, these results indicate that the amygdala has a facilitating role in social play, receiving environmental information and modulating playful activities (Siviy and Panksepp 2011; Trezza et al. 2012). The present study shows that during play behaviour, cellular activity in the mPFC and OFC is correlated with activity in the amygdala, which supports the hypothesis that cortico-amygdala connections are important for social play behaviour. In addition, the correlations observed in the present study between the amygdala and ventral striatum regions as well as the known role of these structures in reward processes (Baxter and Murray 2002; Berridge and Kringelbach 2008; Cardinal et al. 2002; Morrison and Salzman 2010), suggest an involvement of amygdalo-striatal connections in the rewarding aspects of social play behaviour.

Thalamus

Social play increased c-Fos expression in the PC, lateral IMDl, and PV thalamic nuclei. The enhancement of the FpCD in these regions was equally distributed over the different intensity categories, suggesting that a new population of cells was recruited by social play in these areas. In addition, a correlation between the PC and its striatal target region and the IMDl and its cortical target region was observed in the play group. A previous study, investigating the involvement of these regions in social play behaviour using c-Fos immunohistochemistry, measured the MD and the midline and intralaminar thalamic nuclei as a whole and did not observe c-Fos activation after play (Gordon et al. 2002), which could be caused by a heterogeneous response of the various subnuclei.

Lesions of the dorsomedial thalamus, posterior thalamus and the parafascicular region of the thalamus have been found to decrease social play behaviour (Siviy and Panksepp 1985, 1987). This has led to the hypothesis that the thalamic nuclei serve as an important relay station in the processing of information to the striatum and prefrontal cortex during social play behaviour (Siviy and Panksepp 2011). In addition, the intralaminar and midline thalamic nuclei are known to have a central role in arousal and attention processes (Groenewegen and Berendse 1994). The present study indicates a specific and discrete activation in the midline and intralaminar thalamic nuclei after play, which may be related to an aroused state required for social play behaviour.

The intralaminar and midline thalamic nuclei have strong topographically organized projections towards the striatum and prefrontal cortex (Groenewegen and Witter 2004; Voorn et al. 2004), regions that were highly activated by play in the present study. However, few correlations were observed between the thalamus and its striatal and prefrontal projection regions. Apparently, the discrete projections originating from the thalamus are not decisive for the neuronal activity patterns in the prefrontal cortex and striatum. Further detailed manipulations of its subnuclei are required to better understand the role of the thalamus in social play behaviour, not least since little is

known regarding the behavioural function of the individual thalamo-cortico-striatal circuits (Groenewegen and Berendse 1994).

Striatal output structures

Besides the several striatal input structures, striatal output structures were also investigated. In the lateral globus pallidus (lGP), a significant decrease in the FpCD was observed after play behaviour. According to basal ganglia connectivity concepts (Gerfen 2004), this is in line with the large increase in FpCD observed in the striatum, which has strong GABAergic projections towards the lGP. Activity in the lGP did not correlate with the activity in any of the striatal regions, however. This may be explained by the fact that the c-Fos activity was determined in the lGP as a whole and not in subregions which are known to receive projections from the striatum in a topographic pattern (Gerfen 2004).

In the ventral pallidum, no effects were observed on the FpCD, although the c-Fos activity in this region did correlate with several of the medial and ventral striatal regions, including the NaCore and NaShell. The fact that these correlations were positive makes it difficult to interpret the correlation in terms of functional changes restricted to the nucleus accumbens to VP projections, which are GABAergic (Gerfen 2004). However, a seemingly paradoxical positive correlation between striatal and pallidal activity has previously been observed in studies examining the effect of dopamine depletion on striatopallidal function (Chesselet and Delfs 1996). Instead of decreased activity in lGP upon activation of striatal input to the nucleus—as would be predicted by current basal ganglia models—an increase in deoxyglucose uptake and in metabolic activity of lGP GABAergic neurons was seen. This has been suggested to be caused by major changes in pallidal firing patterns and GABAergic neurotransmission in lGP. Interestingly, in the present experiments the correlations turned from negative to positive in non-playing vs. playing animals, respectively. This suggests a particular functional involvement of the ventral pallidum during play behaviour.

The SNr is another important output structure of the striatum. It is known that the SNr receives major GABA-ergic outputs from the striatum (Gerfen 2004). However, in the present study a positive correlation was observed with the mCore in the play group and the lCore in the no-play group. By analogy to the correlation between VP and nucleus accumbens discussed above, such a positive correlation may be explained by changes in GABAergic activity in SNr that occur as a consequence of striatal activity. However, an alternative explanation may be that other than striatal inputs to pallidum or SNr contribute to the c-Fos activity observed in these regions. For example,

considering the lGP and VP, it may be that a sub-threshold, viz. non-significant, change in FpCD occurs in a subpopulation of neurons that is contacted by sources other than the striatum, such as the cortex or subthalamic nucleus (Voorn 2010).

Monoamine nuclei and related regions

Social play behaviour did not detectably enhance the levels of c-Fos in the VTA and SN. Considering the major role of dopamine in motivational processes (Berridge 2007; Robbins and Everitt 2007; Salamone et al. 2005), this was an unexpected result. However, the involvement of dopaminergic neurotransmission in social play behaviour is not straightforward. Thus, augmenting dopaminergic neurotransmission using receptor agonists or reuptake blockers does not invariably lead to increases in social play. In fact, modest increases as well as decreases have been found (Beatty et al. 1984; Niesink and Van Ree 1989; Siviy et al. 1996; Vanderschuren et al. 2008). Possibly, social play behaviour recruits only a small subset of dopaminergic neurons, which results in activation below the detection limit. Indeed, the anatomical organization of the VTA is highly heterogeneous (Ikemoto 2007).

Despite the absence of a significant effect of play on c-Fos activity as such, correlations were observed between the VTA/SN regions and their corticostriatal target regions. The VTA and SN provide a dopaminergic projection to the prefrontal cortex and striatum and this output is reciprocated by GABAergic and glutamatergic inputs from these regions (Gerfen et al. 1987; Gerfen 2004; Lammel et al. 2008, 2011). Regarding the prefrontal cortex, the VTA showed correlations with all the mPFC regions and the ventrolateral orbitofrontal region, the latter being surprising considering the low number of dopamine fibres in the VLO (Van De Werd and Uylings 2008). The VTA mainly projects to the more ventral parts of the striatum (Gerfen et al. 1987; Lammel et al. 2011) and correlations were observed between the VTA and NaShell and olfactory tubercle. In contrast, correlations between the SNc and striatum and prefrontal cortex were not widespread, suggesting that the increased SNc activity is not a main contributor to c-Fos activity in the striatum. These results suggest that the dopaminergic modulation of the striatum and prefrontal cortex from the VTA plays a role in social play behaviour. It is likely that these projections are important for motivational and cognitive control aspects of social play behaviour, mediated by the ventral striatum and prefrontal cortex, respectively (Berridge 2007; Dalley et al. 2004; Ikemoto and Panksepp 1999; Robbins and Everitt 2007; Robbins and Arnsten 2009; Salamone et al. 2005; Seamans and Yang 2004).

Induction of c-Fos activity after play was observed in the DR, which fits with the involvement of serotonin in social play behaviour (Homberg et al. 2007; Siviy et al. 2011; Vanderschuren et al. 1997). The mechanism by which serotonin modulates social play behaviour is not completely understood, due to the high complexity and widespread distribution of serotonin receptors, but this induction of c-Fos expression in the DR is supportive of a role for the serotonin system in social play.

Social play behaviour did not induce c-Fos expression in the LC, despite the known involvement of noradrenaline in social play behaviour (Trezza et al. 2010; Vanderschuren et al. 2008). Enhancement of endogenous noradrenaline levels has been shown to disrupt social play behaviour (Vanderschuren et al. 2008), suggesting that high levels of noradrenaline and social play are incompatible. It is possible that during social play behaviour, the release of noradrenaline is limited by the LC and therefore no c-Fos induction is observed in this region. Generally, basal c-Fos levels are low and as a consequence reductions in c-Fos levels are difficult to detect (Kovacs 2008).

With respect to regions of the tegmentum that regulate activity in the monoamine nuclei, the RMTg did not show an overall increase in FpCD, while more cells were detected in the dark intensity category, suggesting that the same population of neurons expressed more c-Fos after social play behaviour. In the PPTg, a new population of cells may be recruited by social play behaviour, since an overall increase in FpCD was observed which was not dependent on intensity levels of the cells. The RMTg has recently received a great deal of attention regarding its role in regulating the activity of VTA dopamine neurons, whereby increased activity of the RMTg results in inhibition of dopaminergic neurons (Hong et al. 2011; Barrot et al. 2012; Jhou et al. 2009a, b). However, since the RMTg also targets other regions (Barrot et al. 2012; Jhou et al. 2009b), and the identity of the c-Fos positive neurons in the RMTg is at present unknown, the implications of these changes in RMTg activity for social play remain as yet unclear.

Besides in the RMTg, social play behaviour induced c-Fos expression in the PPTg, while no changes were observed in the LDTg. The PPTg and LDTg provide cholinergic and glutamatergic projections towards the dopamine producing regions, where axons from the PPTg mainly reach the SNc and those from the LDTg mainly target the VTA (Forster and Blaha 2000; Holmstrand and Sesack 2011). Both regions are important for regulating the activity of dopaminergic neurons, where activity in these regions is thought to enhance dopamine release (Blaha and Winn 1993; Blaha et al. 1996). The increased c-Fos expression observed in the PPTg after social play behaviour, may therefore be related to its function in regulating dopamine activity.

Concluding remarks

The current study shows that social play behaviour induced cellular activity in a wide array of neural structures, which is consistent with the complex nature of this behaviour. Previous immediate early gene expression studies investigated a number of regions that were also investigated in our study. Consistent activation was observed after play behaviour in dorsal and ventral striatum (Gordon et al. 2002), AC, PrL, IL and BNST (Cheng et al. 2008). Contrasting results compared to the present study were reported for the MeA, where Cheng et al. (2008) observed an increase in activity and the AC, OFC, and dorsomedial thalamus where Gordon et al. (2002) observed no changes. These discrepancies may be related to experimental differences between the studies. First, the study by Cheng et al. (2008) investigated social play behaviour in golden hamsters, whereas Gordon et al. (2002) and the present study used rats. Given the subtle differences in the structure of social play behaviour between rodent species (Pellis and Pellis 1998), it is conceivable that the neural substrates of social play behaviour in rats and hamsters somewhat differ. The absence of an increase in the AC, OFC, and thalamus after social play behaviour in the Gordon et al. (2002) study may be related to the fact that in that study a portion of these regions using a rectangle or circle template was measured, whereas in the present study the AC, OFC and thalamus subregions were measured separately and the borders of these regions were defined according to adjacent Nissl-stained sections. Lastly, both Gordon et al. (2002) and Cheng et al. (2008) detected c-Fos protein levels using immunohistochemistry, whereas in the present study c-Fos mRNA levels were measured by in situ hybridisation. Thus, the differences in the results may also be related to distinct effects of social play on c-Fos mRNA expression versus Fos protein levels.

In the present study, the neural substrates of social play behaviour were investigated in male rats. The structure and intensity of social play behaviour in rats somewhat differ between males and females (Pellis et al. 1997). It is therefore well conceivable that social play behaviour in female rats relies on activity in a neural network, that is not identical to the network in male rats identified here, even if it is likely that there is substantial overlap between the neural substrates of social play in male and female rats.

In conclusion, the present study substantially furthers our knowledge on the neural substrates of social play behaviour by investigating a large number of brain regions that may be relevant to social play. The changes in c-Fos expression induced by social play behaviour were analysed in considerable anatomical detail, allowing for the detection of subregional differences in social play-induced neuronal activity. Relationships in social play-induced

cellular activity between connected regions were also taken into account, leading us to propose a potential neural network of social play behaviour as presented in Fig. 12. These data indicate that activity of corticostriatal systems, together with the amygdala and monoaminergic systems, underlies social play. By demonstrating how several interconnected systems in the brain are involved in this behaviour, the present study provides an elaborate starting point for functional investigations aimed at improving our understanding of the neurobiology of social play behaviour.

References

Alessandri SM (1992) Attention, play, and social behavior in ADHD preschoolers. J Abnorm Child Psychol 20:289–302

Alheid GF (2003) Extended amygdala and basal forebrain. Ann N Y Acad Sci 985:185–205

Baarendse PJJ, Counotte DS, O'Donnell P, Vanderschuren LJMJ (2013) Social experience during adolescence is critical for the development of cognitive control and dopamine modulation of prefrontal cortex function. Neuropsychopharmacology. doi:10.1038/npp.2013.47

Badiani A, Oates MM, Day HEW, Watson SJ, Akil H, Robinson TE (1998) Amphetamine-induced behavior, dopamine release, and c-Fos mRNA expression: modulation by environmental novelty. J Neurosci 18:10579–10593

Balleine BW, Liljeholm M, Ostlund SB (2009) The integrative function of the basal ganglia in instrumental conditioning. Behav Brain Res 199:43–52

Barrot M, Sesack SR, Georges F, Pistis M, Hong S, Jhou TC (2012) Braking dopamine systems: a new GABA master structure for mesolimbic and nigrostriatal functions. J Neurosci 32:14094–14101

Baxter MG, Murray EA (2002) The amygdala and reward. Nat Rev Neurosci 3:563–573

Beatty WW, Costello KB, Berry SL (1984) Suppression of play fighting by amphetamine: effects of catecholamine antagonists, agonists and synthesis inhibitors. Pharmacol Biochem Behav 20:747–755

Bell HC, McCaffrey DR, Forgie ML, Kolb B, Pellis SM (2009) The role of the medial prefrontal cortex in the play fighting of rats. Behav Neurosci 123:1158–1168

Bell HC, Pellis SM, Kolb B (2010) Juvenile peer play experience and the development of the orbitofrontal and medial prefrontal cortices. Behav Brain Res 207:7–13

Berridge KC (2007) The debate over dopamine's role in reward: the case for incentive salience. Psychopharmacology 191:391–431

Berridge KC, Kringelbach ML (2008) Affective neuroscience of pleasure: reward in humans and animals. Psychopharmacology 199:457–480

Blaha CD, Winn P (1993) Modulation of dopamine efflux in the striatum following cholinergic stimulation of the substantia nigra in intact and pedunculopontine tegmental nucleus-lesioned rats. J Neurosci 13:1035–1044

Blaha CD, Allen LF, Das S, Inglis WL, Latimer MP, Vincent SR, Winn P (1996) Modulation of dopamine efflux in the nucleus accumbens after cholinergic stimulation of the ventral tegmental area in intact, pedunculopontine tegmental nucleus-lesioned, and laterodorsal tegmental nucleus-lesioned rats. J Neurosci 16:714–722

Blakemore SJ (2008) The social brain in adolescence. Nat Rev Neurosci 9:267–277

Braun K, Bock J (2011) The experience-dependent maturation of prefronto-limbic circuits and the origin of developmental psychopathology: implications for the pathogenesis and therapy of behavioural disorders. Dev Med Child Neurol 53(Suppl 4):14–18

Cardinal RN, Parkinson JA, Hall J, Everitt BJ (2002) Emotion and motivation: the role of the amygdala, ventral striatum, and prefrontal cortex. Neurosci Biobehav Rev 26:321–352

Cassell MD, Wright DJ (1986) Topography of projections from the medial prefrontal cortex to the amygdala in the rat. Brain Res Bull 17:321–333

Cheng SY, Taravosh-Lahn K, Delville Y (2008) Neural circuitry of play fighting in golden hamsters. Neuroscience 156:247–256

Chesselet MF, Delfs JM (1996) Basal ganglia and movement disorders: an update. Trends Neurosci 19:417–422

Christakou A, Robbins TW, Everitt BJ (2001) Functional disconnection of a prefrontal cortical-dorsal striatal system disrupts choice reaction time performance: implications for attentional function. Behav Neurosci 115:812–825

Christakou A, Robbins TW, Everitt BJ (2004) Prefrontal cortical-ventral striatal interactions involved in affective modulation of attentional performance: implications for corticostriatal circuit function. J Neurosci 24:773–780

Churchwell JC, Morris AM, Heurtelou NM, Kesner RP (2009) Interactions between the prefrontal cortex and amygdala during delay discounting and reversal. Behav Neurosci 123:1185–1196

Crone EA, Dahl RE (2012) Understanding adolescence as a period of social-affective engagement and goal flexibility. Nat Rev Neurosci 13:636–650

Cullinan WE, Herman JP, Battaglia DF, Akil H, Watson SJ (1995) Pattern and time course of immediate early gene expression in rat brain following acute stress. Neuroscience 64:477–505

Daenen EW, Wolterink G, Gerrits MAFM, Van Ree JM (2002) The effects of neonatal lesions in the amygdala or ventral hippocampus on social behaviour later in life. Behav Brain Res 136:571–582

Dalley JW, Cardinal RN, Robbins TW (2004) Prefrontal executive and cognitive functions in rodents: neural and neurochemical substrates. Neurosci Biobehav Rev 28:771–784

Day HEW, Badiani A, Uslaner JM, Oates MM, Vittoz NM, Robinson TE, Watson SJ Jr, Akil H (2001) Environmental novelty differentially affects c-Fos mRNA expression induced by amphetamine or cocaine in subregions of the bed nucleus of the stria terminalis and amygdala. J Neurosci 21:732–740

Fagen R (1981) Animal play behavior. Oxford University Press, Oxford

Forster GL, Blaha CD (2000) Laterodorsal tegmental stimulation elicits dopamine efflux in the rat nucleus accumbens by activation of acetylcholine and glutamate receptors in the ventral tegmental area. Eur J Neurosci 12:3596–3604

Gerfen CR (2004) Basal ganglia. In: Paxinos G (ed) The rat nervous system. Academic Press, San Diego, pp 455–508

Gerfen CR, Herkenham M, Thibault J (1987) The neostriatal mosaic: II. Patch- and matrix-directed mesostriatal dopaminergic and non-dopaminergic systems. J Neurosci 7:3915–3934

Gordon NS, Kollack-Walker S, Akil H, Panksepp J (2002) Expression of c-Fos gene activation during rough and tumble play in juvenile rats. Brain Res Bull 57:651–659

Graham KL, Burghardt GM (2010) Current perspectives on the biological study of play: signs of progress. Q Rev Biol 85:393–418

Groenewegen HJ, Berendse HW (1994) The specificity of the 'nonspecific' midline and intralaminar thalamic nuclei. Trends Neurosci 17:52–57

Groenewegen HJ, Uylings HBM (2010) Organization of prefrontal-striatal projections. In: Steiner H, Tseng KY (eds) Handbook of basal ganglia structure and function. Academic Press, London, pp 353–365

Groenewegen HJ, Witter MP (2004) Thalamus. In: Paxinos G (ed) The rat nervous system. Academic Press, San Diego, pp 407–453

Haber SN, Knutson B (2010) The reward circuit: linking primate anatomy and human imaging. Neuropsychopharmacology 35:4–26

Higo N, Oishi T, Yamashita A, Matsuda K, Hayashi M (1999) Quantitative non-radioactive in situ hybridization study of GAP-43 and SCG10 mRNAs in the cerebral cortex of adult and infant macaque monkeys. Cereb Cortex 9:317–331

Hill WD, Arai M, Cohen JA, Trojanowski JQ (1993) Neurofilament mRNA is reduced in Parkinson's disease substantia nigra pars compacta neurons. J Comp Neurol 329:328–336

Holmstrand EC, Sesack SR (2011) Projections from the rat pedunculopontine and laterodorsal tegmental nuclei to the anterior thalamus and ventral tegmental area arise from largely separate populations of neurons. Brain Struct Funct 216:331–345

Homberg JR, Schiepers OJG, Schoffelmeer ANM, Cuppen E, Vanderschuren LJMJ (2007) Acute and constitutive increases in central serotonin levels reduce social play behaviour in peri-adolescent rats. Psychopharmacology 195:175–182

Hong S, Jhou TC, Smith M, Saleem KS, Hikosaka O (2011) Negative reward signals from the lateral habenula to dopamine neurons are mediated by rostromedial tegmental nucleus in primates. J Neurosci 31:11457–11471

Ikemoto S (2007) Dopamine reward circuitry: two projection systems from the ventral midbrain to the nucleus accumbens–olfactory tubercle complex. Brain Res Rev 56:27–78

Ikemoto S, Panksepp J (1999) The role of nucleus accumbens dopamine in motivated behavior: a unifying interpretation with special reference to reward-seeking. Brain Res Brain Res Rev 31:6–41

Jhou TC, Fields HL, Baxter MG, Saper CB, Holland PC (2009a) The rostromedial tegmental nucleus (RMTg), a GABAergic afferent to midbrain dopamine neurons, encodes aversive stimuli and inhibits motor responses. Neuron 61:786–800

Jhou TC, Geisler S, Marinelli M, Degarmo BA, Zahm DS (2009b) The mesopontine rostromedial tegmental nucleus: a structure targeted by the lateral habenula that projects to the ventral tegmental area of Tsai and substantia nigra compacta. J Comp Neurol 513:566–596

Jordan R (2003) Social play and autistic spectrum disorders: a perspective on theory, implications and educational approaches. Autism 7:347–360

Kelley AE (2004) Ventral striatal control of appetitive motivation: role in ingestive behavior and reward-related learning. Neurosci Biobehav Rev 27:765–776

Kelley AE, Domesick VB, Nauta WJH (1982) The amygdalostriatal projection in the rat—an anatomical study by anterograde and retrograde tracing methods. Neuroscience 7:615–630

Kovacs KJ (2008) Measurement of immediate-early gene activation-c-Fos and beyond. J Neuroendocrinol 20:665–672

Lammel S, Hetzel A, Hackel O, Jones I, Liss B, Roeper J (2008) Unique properties of mesoprefrontal neurons within a dual mesocorticolimbic dopamine system. Neuron 57:760–773

Lammel S, Ion DI, Roeper J, Malenka RC (2011) Projection-specific modulation of dopamine neuron synapses by aversive and rewarding stimuli. Neuron 70:855–862

Lewis KP, Barton RA (2006) Amygdala size and hypothalamus size predict social play frequency in nonhuman primates: a comparative analysis using independent contrasts. J Comp Psychol 120:31–37

Manning MM, Wainwright LD (2010) The role of high level play as a predictor social functioning in autism. J Autism Dev Disord 40:523–533

Maren S, Quirk GJ (2004) Neuronal signalling of fear memory. Nat Rev Neurosci 5:844–852

McDonald AJ, Mascagni F, Guo L (1996) Projections of the medial and lateral prefrontal cortices to the amygdala: a Phaseolus vulgaris leucoagglutinin study in the rat. Neuroscience 71:55–75

McFarland K, Lapish CC, Kalivas PW (2003) Prefrontal glutamate release into the core of the nucleus accumbens mediates cocaine-induced reinstatement of drug-seeking behavior. J Neurosci 23:3531–3537

Meaney MJ, Dodge AM, Beatty WW (1981) Sex-dependent effects of amygdaloid lesions on the social play of prepubertal rats. Physiol Behav 26:467–472

Miyachi S, Hasegawa YT, Gerfen CR (2005) Coincident stimulation of convergent cortical inputs enhances immediate early gene induction in the striatum. Neuroscience 134:1013–1022

Morgan JI, Curran T (1991) Stimulus–transcription coupling in the nervous system: involvement of the inducible proto-oncogenes fos and jun. Annu Rev Neurosci 14:421–451

Morrison SE, Salzman CD (2010) Re-valuing the amygdala. Curr Opin Neurobiol 20:221–230

Nelson EE, Leibenluft E, McClure EB, Pine DS (2005) The social re-orientation of adolescence: a neuroscience perspective on the process and its relation to psychopathology. Psychol Med 35:163–174

Niesink RJM, Van Ree JM (1989) Involvement of opioid and dopaminergic systems in isolation-induced pinning and social grooming of young rats. Neuropharmacology 28:411–418

Nordquist RE, Vanderschuren LJMJ, Jonker AJ, Bergsma M, De Vries TJ, Pennartz CMA, Voorn P (2008) Expression of amphetamine sensitization is associated with recruitment of a reactive neuronal population in the nucleus accumbens core. Psychopharmacology 198:113–126

Ostrander MM, Badiani A, Day HEW, Norton CS, Watson SJ, Akil H, Robinson TE (2003) Environmental context and drug history modulate amphetamine-induced c-Fos mRNA expression in the basal ganglia, central extended amygdala, and associated limbic forebrain. Neuroscience 120:551–571

Panksepp J, Siviy S, Normansell L (1984) The psychobiology of play: theoretical and methodological perspectives. Neurosci Biobehav Rev 8:465–492

Panksepp J, Normansell L, Cox JF, Siviy SM (1994) Effects of neonatal decortication on the social play of juvenile rats. Physiol Behav 56:429–443

Parkinson JA, Willoughby PJ, Robbins TW, Everitt BJ (2000) Disconnection of the anterior cingulate cortex and nucleus accumbens core impairs Pavlovian approach behavior: further evidence for limbic cortical-ventral striatopallidal systems. Behav Neurosci 114:42–63

Parthasarathy HB, Graybiel AM (1997) Cortically driven immediate-early gene expression reflects modular influence of sensorimotor cortex on identified striatal neurons in the squirrel monkey. J Neurosci 17:2477–2491

Paus T, Keshavan M, Giedd JN (2008) Why do many psychiatric disorders emerge during adolescence? Nat Rev Neurosci 9:947–957

Paxinos G, Watson C (1998) The rat brain in sterotaxic coordinates. Academic Press, San Diego

Pellis SM, Pellis VC (1998) Play fighting of rats in comparative perspective: a schema for neurobehavioral analyses. Neurosci Biobehav Rev 23:87–101

Pellis SM, Pellis VC (2007) Rough-and-tumble play and the development of the social brain. Curr Direct Psychol Sci 16:95–98

Pellis SM, Pellis VC (2009) The playful brain. OneWorld Publications, Oxford, UK

Pellis SM, Pellis VC, Whishaw IQ (1992) The role of the cortex in play fighting by rats: developmental and evolutionary implications. Brain Behav Evol 39:270–284

Pellis SM, Castaneda E, McKenna MM, Tran-Nguyen LT, Whishaw IQ (1993) The role of the striatum in organizing sequences of play fighting in neonatally dopamine-depleted rats. Neurosci Lett 158:13–15

Pellis SM, Field EF, Smith LK, Pellis VC (1997) Multiple differences in the play fighting of male and female rats. Implications for the causes and functions of play. Neurosci Biobehav Rev 21:105–120

Pellis SM, Hastings E, Shimizu T, Kamitakahara H, Komorowska J, Forgie ML, Kolb B (2006) The effects of orbital frontal cortex damage on the modulation of defensive responses by rats in playful and nonplayful social contexts. Behav Neurosci 120:72–84

Phelps EA, Ledoux JE (2005) Contributions of the amygdala to emotion processing: from animal models to human behavior. Neuron 48:175–187

Robbins TW, Arnsten AF (2009) The neuropsychopharmacology of fronto-executive function: monoaminergic modulation. Annu Rev Neurosci 32:267–287

Robbins TW, Everitt BJ (2007) A role for mesencephalic dopamine in activation: commentary on Berridge (2006). Psychopharmacology 191:433–437

Robbins E, Baldino F Jr, Roberts-Lewis JM, Meyer SL, Grega D, Lewis ME (1991) Quantitative non-radioactive in situ hybridization of preproenkephalin mRNA with digoxigenin-labeled cRNA probes. Anat Rec 231:559–562

Rozen S, Skaletsky HJ (2000) Primer3 on the WWW for general users and for biologist programmers. In: Krawetz S, Misener S (eds) Bioinformatics methods and protocols: methods in molecular biology. Humana Press, Totowa, pp 365–386

Salamone JD, Correa M, Mingote SM, Weber SM (2005) Beyond the reward hypothesis: alternative functions of nucleus accumbens dopamine. Curr Opin Pharmacol 5:34–41

Schilling K, Curran T, Morgan JI (1991) Fosvergnügen. The excitement of immediate-early genes. Ann N Y Acad Sci 627:115–123

Schilman EA, Uylings HB, Galis-de Graaf Y, Joel D, Groenewegen HJ (2008) The orbital cortex in rats topographically projects to central parts of the caudate–putamen complex. Neurosci Lett 432:40–45

Schneider M, Koch M (2005) Deficient social and play behavior in juvenile and adult rats after neonatal cortical lesion: effects of chronic pubertal cannabinoid treatment. Neuropsychopharmacology 30:944–957

Schoenbaum G, Setlow B, Saddoris MP, Gallagher M (2003) Encoding predicted outcome and acquired value in orbitofrontal cortex during cue sampling depends upon input from basolateral amygdala. Neuron 39:855–867

Seamans JK, Yang CR (2004) The principal features and mechanisms of dopamine modulation in the prefrontal cortex. Prog Neurobiol 74:1–58

Sesack SR, Grace AA (2010) Cortico-basal ganglia reward network: microcircuitry. Neuropsychopharmacology 35:27–47

Siviy SM, Panksepp J (1985) Dorsomedial diencephalic involvement in the juvenile play of rats. Behav Neurosci 99:1103–1113

Siviy SM, Panksepp J (1987) Juvenile play in the rat: thalamic and brain stem involvement. Physiol Behav 41:103–114

Siviy SM, Panksepp J (2011) In search of the neurobiological substrates for social playfulness in mammalian brains. Neurosci Biobehav Rev 35:1821–1830

Siviy SM, Fleischhauer AE, Kerrigan LA, Kuhlman SJ (1996) D2 dopamine receptor involvement in the rough-and-tumble play behavior of juvenile rats. Behav Neurosci 110:1168–1176

Siviy SM, Deron LM, Kasten CR (2011) Serotonin, motivation, and playfulness in the juvenile rat. Dev Cogn Neurosci 1:606–616

Spear LP (2000) The adolescent brain and age-related behavioral manifestations. Neurosci Biobehav Rev 24:417–463

Špinka M, Newberry RC, Bekoff M (2001) Mammalian play: training for the unexpected. Q Rev Biol 76:141–168

Struthers WM, DuPriest A, Runyan J (2005) Habituation reduces novelty-induced FOS expression in the striatum and cingulate cortex. Exp Brain Res 167:136–140

Stylianopoulou E, Lykidis D, Ypsilantis P, Simopoulos C, Skavdis G, Grigoriou M (2012) A rapid and highly sensitive method of non radioactive colorimetric in situ hybridization for the detection of mRNA on tissue sections. PLoS ONE 7:e33898

Trezza V, Vanderschuren LJMJ (2008) Cannabinoid and opioid modulation of social play behavior in adolescent rats: differential behavioral mechanisms. Eur Neuropsychopharmacol 18:519–530

Trezza V, Baarendse PJJ, Vanderschuren LJMJ (2009) Prosocial effects of nicotine and ethanol in adolescent rats through partially dissociable neurobehavioral mechanisms. Neuropsychopharmacology 34:2560–2573

Trezza V, Baarendse PJJ, Vanderschuren LJMJ (2010) The pleasures of play: pharmacological insights into social reward mechanisms. Trends Pharmacol Sci 31:463–469

Trezza V, Campolongo P, Vanderschuren LJMJ (2011a) Evaluating the rewarding nature of social interactions in laboratory animals. Dev Cogn Neurosci 1:444–458

Trezza V, Damsteegt R, Achterberg EJM, Vanderschuren LJMJ (2011b) Nucleus accumbens mu-opioid receptors mediate social reward. J Neurosci 31:6362–6370

Trezza V, Damsteegt R, Manduca A, Petrosino S, van Kerkhof LWM, Pasterkamp RJ, Zhou Y, Campolongo P, Cuomo V, Di Marzo V, Vanderschuren LJMJ (2012) Endocannabinoids in amygdala and nucleus accumbens mediate social play reward in adolescent rats. J Neurosci 32:14899–14908

Van De Werd HJJM, Uylings HBM (2008) The rat orbital and agranular insular prefrontal cortical areas: a cytoarchitectonic and chemoarchitectonic study. Brain Struct Funct 212:387–401

Van den Berg CL, Hol T, Van Ree JM, Spruijt BM, Everts H, Koolhaas JM (1999) Play is indispensable for an adequate development of coping with social challenges in the rat. Dev Psychobiol 34:129–138

van der Plasse G, Schrama R, van Seters SP, Vanderschuren LJMJ, Westenberg HGM (2012) Deep brain stimulation reveals a dissociation of consummatory and motivated behaviour in the medial and lateral nucleus accumbens shell of the rat. PLoS ONE 7:e33455

Van der Werf YD, Witter MP, Groenewegen HJ (2002) The intralaminar and midline nuclei of the thalamus. Anatomical and functional evidence for participation in processes of arousal and awareness. Brain Res Brain Res Rev 39:107–140

Vanderschuren LJMJ (2010) How the brain makes play fun. Am J Play 2:315–337

Vanderschuren LJMJ, Niesink RJM, Spruijt BM, Van Ree JM (1995a) Influence of environmental factors on social play behavior of juvenile rats. Physiol Behav 58:119–123

Vanderschuren LJMJ, Niesink RJM, Spruijt BM, Van Ree JM (1995b) Effects of morphine on different aspects of social play in juvenile rats. Psychopharmacology 117:225–231

Vanderschuren LJMJ, Niesink RJM, Van Ree JM (1997) The neurobiology of social play behavior in rats. Neurosci Biobehav Rev 21:309–326

Vanderschuren LJMJ, Trezza V, Griffioen-Roose S, Schiepers OJG, Van Leeuwen N, De Vries TJ, Schoffelmeer ANM (2008) Methylphenidate disrupts social play behavior in adolescent rats. Neuropsychopharmacology 33:2946–2956

Von Frijtag JC, Schot M, Van den Bos R, Spruijt BM (2002) Individual housing during the play period results in changed responses to and consequences of a psychosocial stress situation in rats. Dev Psychobiol 41:58–69

Voorn P (2010) Projections from pallidum to striatum. In: Steiner H, Tseng KY (eds) Handbook of basal ganglia structure and function. Academic Press, San Diego, pp 249–257

Voorn P, Vanderschuren LJMJ, Groenewegen HJ, Robbins TW, Pennartz CMA (2004) Putting a spin on the dorsal–ventral divide of the striatum. Trends Neurosci 27:468–474

Watabe-Uchida M, Zhu L, Ogawa SK, Vamanrao A, Uchida N (2012) Whole-brain mapping of direct inputs to midbrain dopamine neurons. Neuron 74:858–873

Willuhn I, Sun W, Steiner H (2003) Topography of cocaine-induced gene regulation in the rat striatum: relationship to cortical inputs and role of behavioural context. Eur J Neurosci 17:1053–1066

Zahm DS (1999) Functional-anatomical implications of the nucleus accumbens core and shell subterritories. Ann N Y Acad Sci 877:113–128

Zhao C, Fujinaga R, Yanai A, Kokubu K, Takeshita Y, Watanabe Y, Shinoda K (2008) Sex-steroidal regulation of aromatase mRNA expression in adult male rat brain: a quantitative non-radioactive in situ hybridization study. Cell Tissue Res 332:381–391